Uncovering doubly charged scalars with dominant three-body decays using machine learning¶

Thomas Flacke

KIAS

KOREA INSTITUTE FOR ADVANCED STUDY
CENTER FOR **ARTIFICIAL INTELLIGENCE** AND **NATURAL SCIENCES**

G. Cacciapaglia, T. Flacke, M. Kunkel, W. Porod, L. Schwarze [JHEP 12 (2022) 087]

T. Flacke, Jeong Han Kim, Pyungwon Ko, M. Kunkel, Jun Seung Pi, W. Porod, L. Schwarze [2304.09195]

… and work in progress

The 3rd International Joint Workshop on the Standard Model and Beyond
and
the 11th KIAS Workshop on Particle Physics and Cosmology,
Jeju 2023/11/13

Outline

- Motivation: Pair-produced scalars are not yet strongly constrained by the LHC. But their signals can be tested.

- A search from doubly charged scalars optimized with Machine Learning

- Conclusion & Outlook

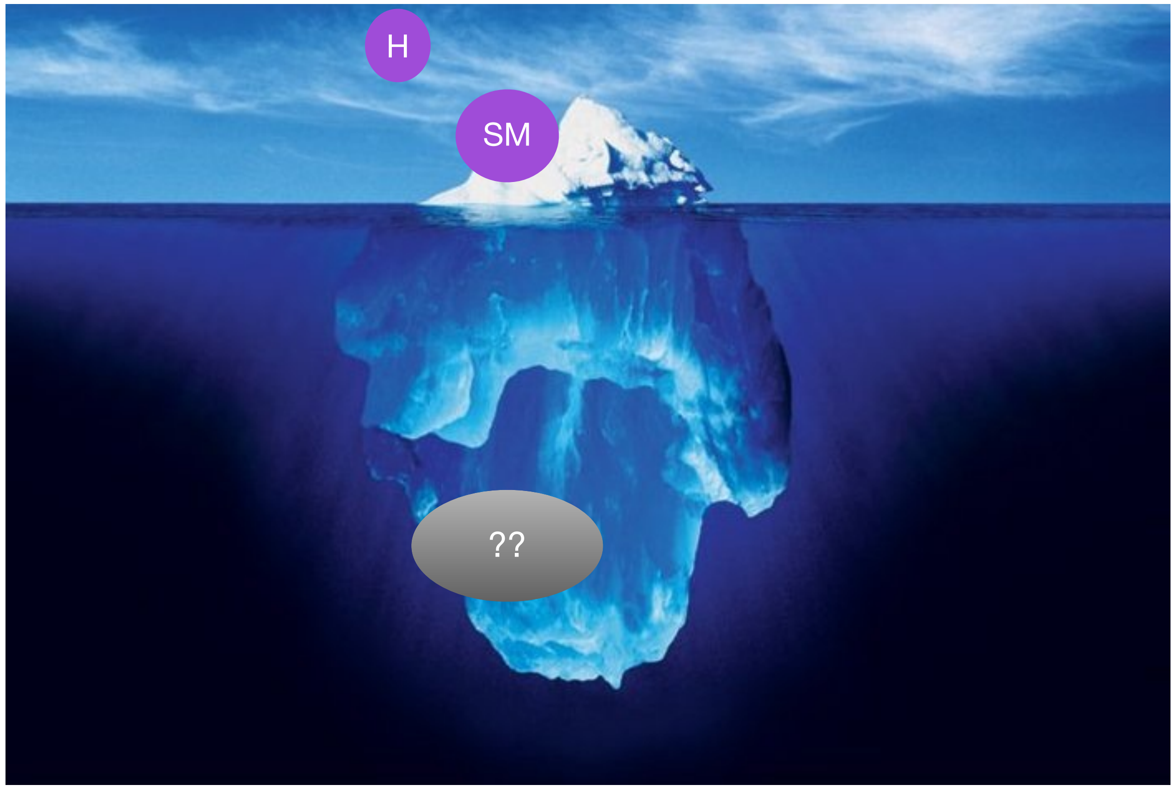

Motivation:
Pair produced BSM scalars

Why is BSM di-scalar production interesting?

- Many SM extensions which address the hierarchy problem have an extended Higgs sector with additional scalars which come in SU(2) multiplets.
- Single-production of BSM scalar interactions is highly model-dependent: arising from
  - Yukawa-type interactions,
  - the scalar kinetic term (if the scalar has a VEV),
  - the potential (via mixing with the Higgs),
  - or generated at loop-level.

  Pair-production is “less model-dependent”:
  The scalar kinetic term yields an SS’V interaction which depends only on the SU(2) x U(1) quantum numbers of the scalar multiplet which guarantees SS’ production through the Drell-Yan process. Mass mixing between different SU(2) multiplets can “re-shuffle” pair-production cross sections, but not tune all pair production cross sections small.

- Final states of scalar single-production are very explicitly targeted by the LHC search program (“resonance searches”). Many final states of scalar pair-production (with $m_S \neq m_H$) are not.

Current bounds on pair produced scalars
all results in one plot

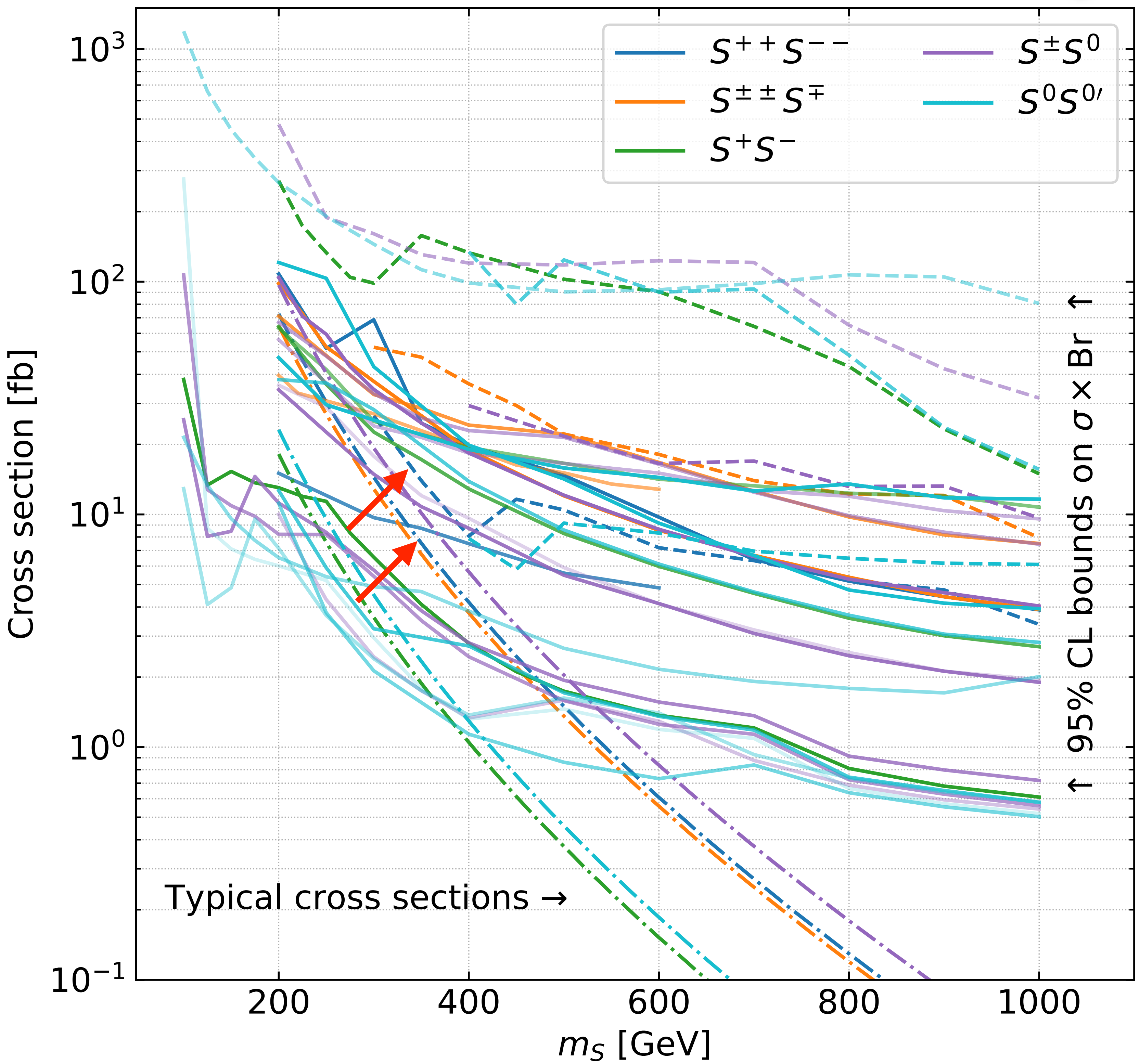

Summary plot

Drell-Yan pair produced scalars: production cross sections for LHC@13 TeV and bounds from recasts of existing searches.

- dash-dotted:
  production cross sections σ
- solid:
  bounds on $\sigma\times$BR(S)$\times$BR(S')
  for decays into EW bosons
- dashed:
  bounds on $\sigma\times$BR(S)$\times$BR(S')
  from recasts for decays into 3rd generation quarks

[JHEP 12 (2022) 087]

Machine Learning applied to di-boson searches: fermiophilic doubly charged scalars [2304.09195]

Event simulation and pre-selection:

- Simulation chain: Feynrules → Madgraph5 → Pythia8 → Delphes3.4.1 →Fastjet3.3.1
- #events
  Signal: 6m events per benchmark mass (300GeV - 800 GeV in 50 GeV steps)
  Background: 4t (4.2m), tth (70m), ttV (150m), ttVV (4.3m), VVV (48m)
- basic selection cuts:
  - exactly 2 same-sign leptons
  - at least 3 b-tagged jets
  - at least 3 (more) jets
  - mild missing p_T cut (20 GeV)
  - mild S_T cut (400 GeV)
  - standard lepton isolation and rapidity criteria (ATLAS config)

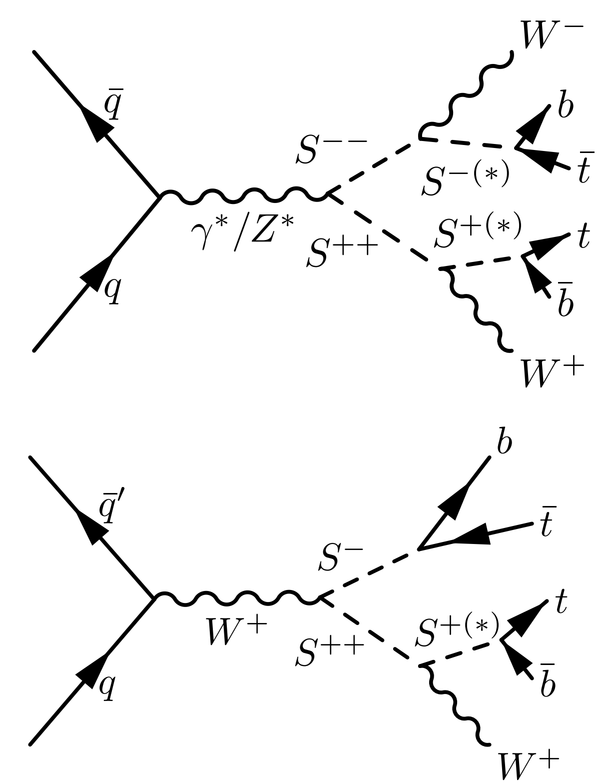

Process	$\epsilon_{\text{Preselection}}$	Cross section [fb]	Events at 3 ab^{-1}
$S^{++}S^{--}$	9.87×10^{-3}	4.90×10^{-2}	147
$S^{\pm\pm}S^{\mp}$	4.81×10^{-3}	2.87×10^{-3}	86
$t\bar{t}V$	1.70×10^{-4}	2.72×10^{-1}	816
$t\bar{t}h$	3.75×10^{-4}	2.10×10^{-1}	629
$t\bar{t}t\bar{t}$	1.63×10^{-2}	1.91×10^{-1}	572
$t\bar{t}VV$	1.74×10^{-3}	3.29×10^{-2}	98
VVV	2.08×10^{-6}	1.05×10^{-3}	3

Table 1. Signal and background efficiencies and cross sections after the preselection cuts. For signal processes, we take the reference pNGB mass to be $m_S = 400$ GeV.

Machine Learning applied to di-boson searches: fermiophilic doubly charged scalars

Data & data-pre-processing

Kinematic data:

We demand 2 leptons, 3 jets, 3 b-jets and construct from them 51 kinematic observables

$$\mathcal{K} = \bigcup_{i \neq j} M_{ij} \cup \bigcup_{i \neq j} \Delta R_{ij} \cup \bigcup_{i} p_{Ti} \cup \{\not{E}_T, S_T\}$$

Jet images:

For each event, we determine an angular maps in the following way:

1. Set the center of the $(\boldsymbol{\eta},\phi)$ plane as the midpoint between the two same-sign leptons.

2. Determine the $(\boldsymbol{\eta},\phi)$ map of the p_T of (a) charged "jets", ((b) neutral "jets",) (c) di-leptons
 by binning objects of the respective class in a 50x50 grid and and summing the p_T in each bin to obtain the pixel intensity
 $\rightarrow \quad V_{\text{image}}^{(C,\ell)} = (2 \times 50 \times 50)$ or $V_{\text{image}}^{(C,N,\ell)} = (3 \times 50 \times 50)$

Machine Learning applied to di-boson searches: fermiophilic doubly charged scalars

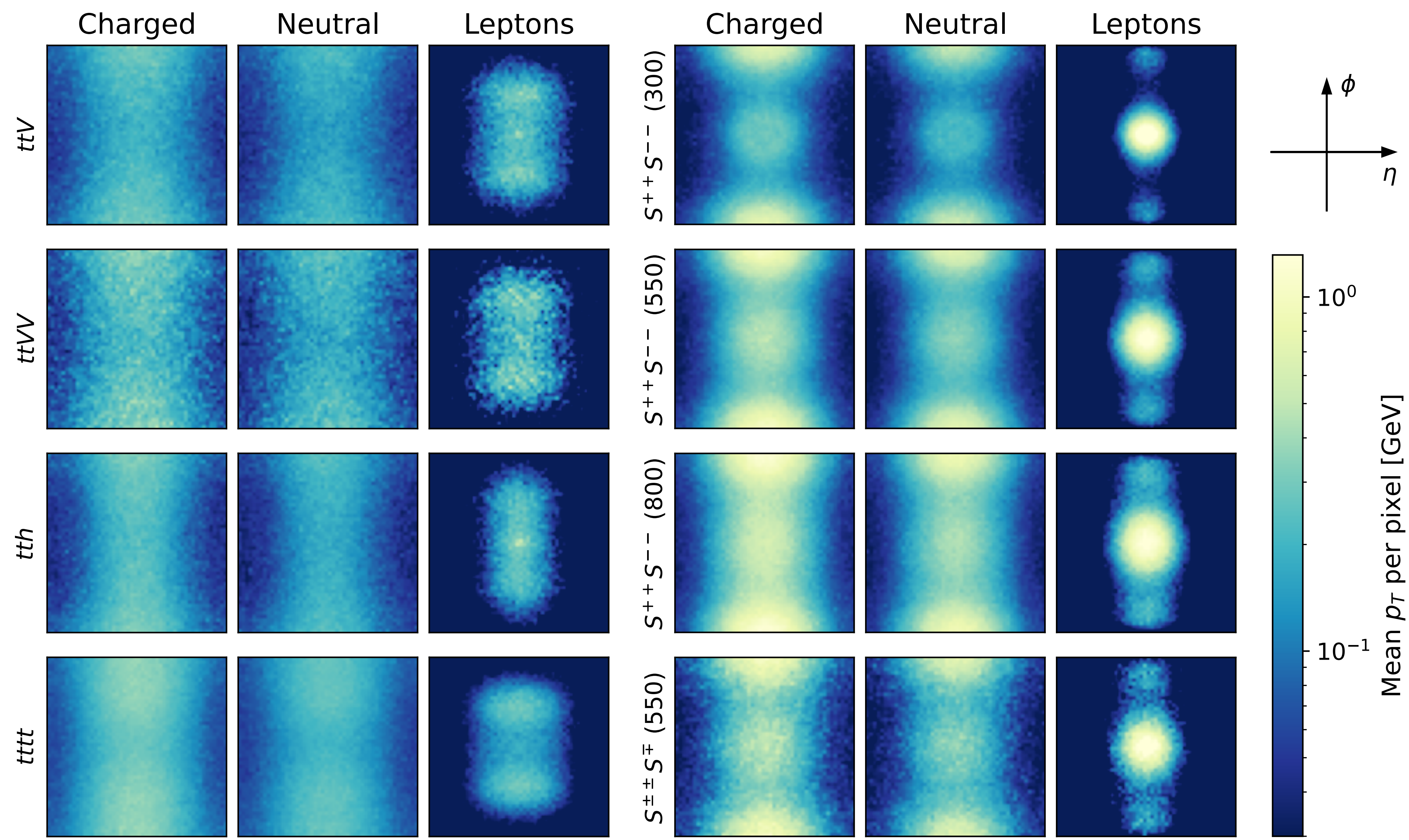

overlaid jet images (various background and signal classes)

Machine Learning applied to di-boson searches: fermiophilic doubly charged scalars

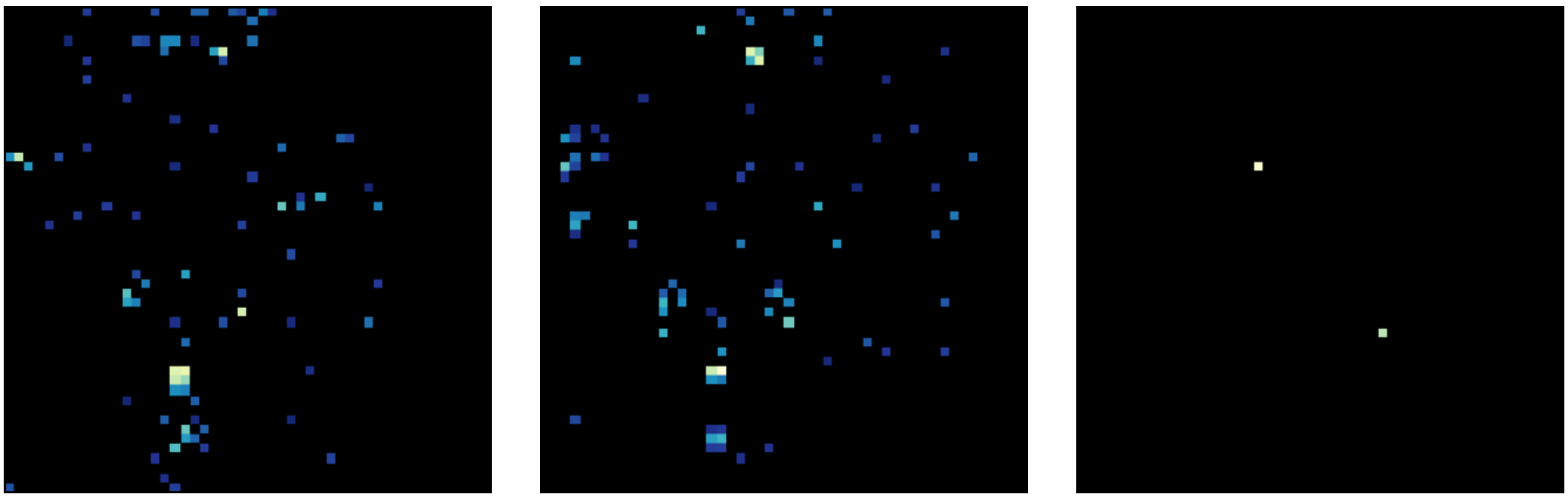

single jet images are sparse

Machine Learning applied to di-boson searches: fermiophilic doubly charged scalars

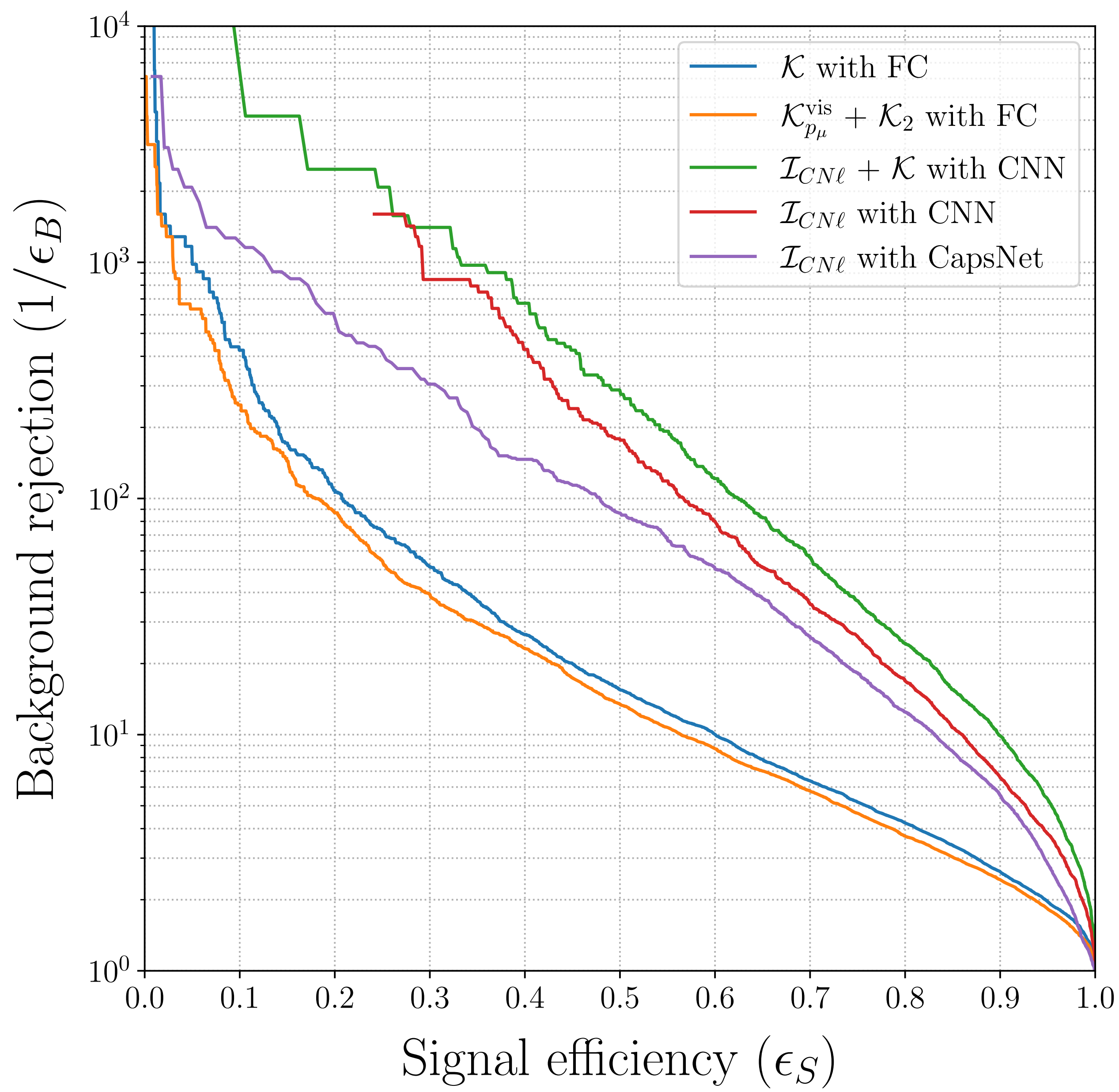

Figure 11. ROC curves for selected NN architectures evaluated on the same test sample.

Machine Learning applied to di-boson searches: fermiophilic doubly charged scalars

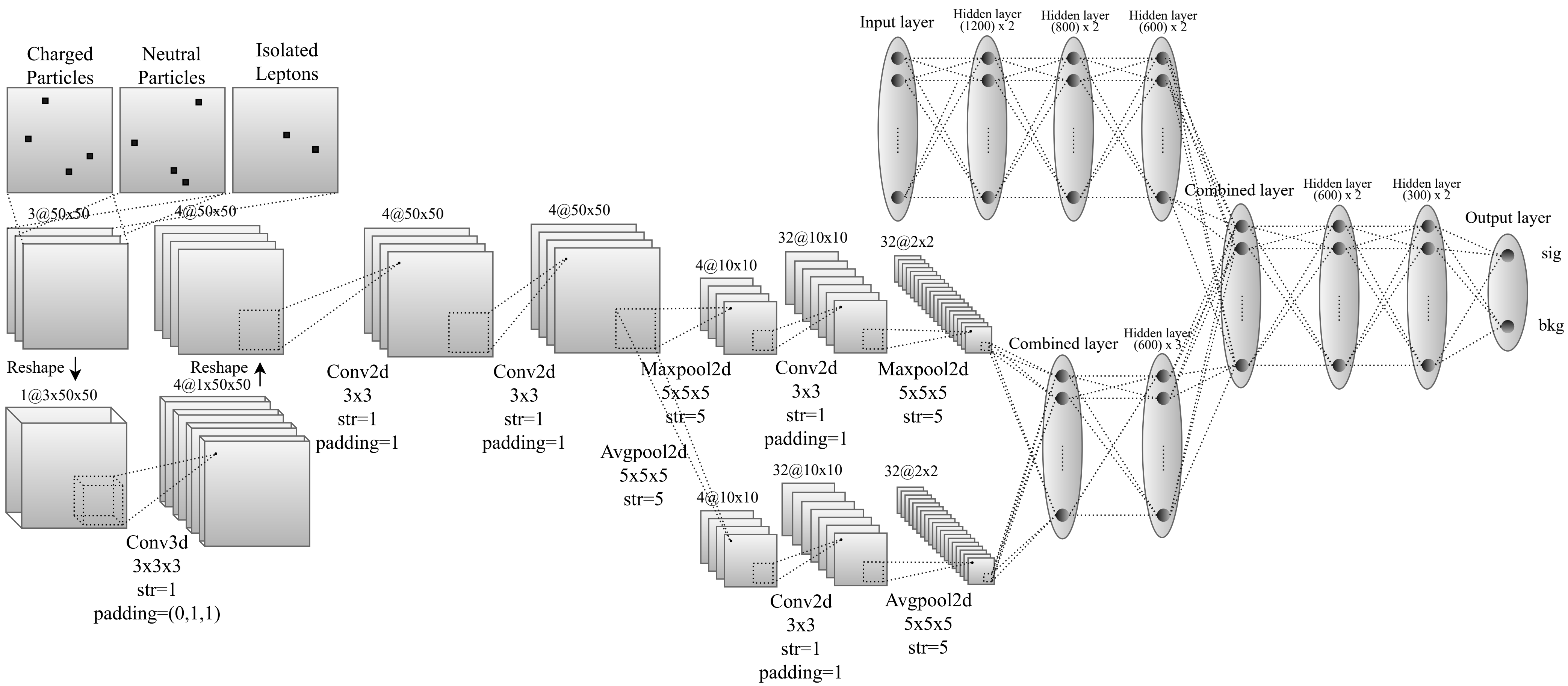

Figure 9. A schematic CNN architecture used in this article. The separate FC chain in the right-upper corner is used only when kinematic variables are included.

Machine Learning applied to di-boson searches: fermiophilic doubly charged scalars

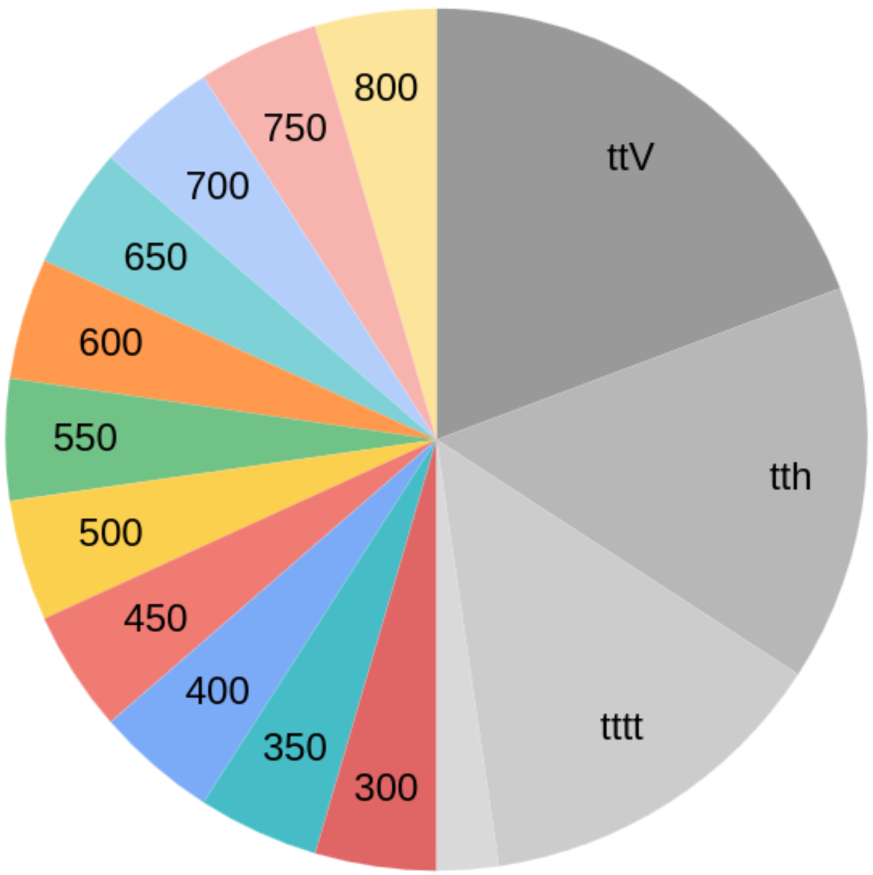

Training

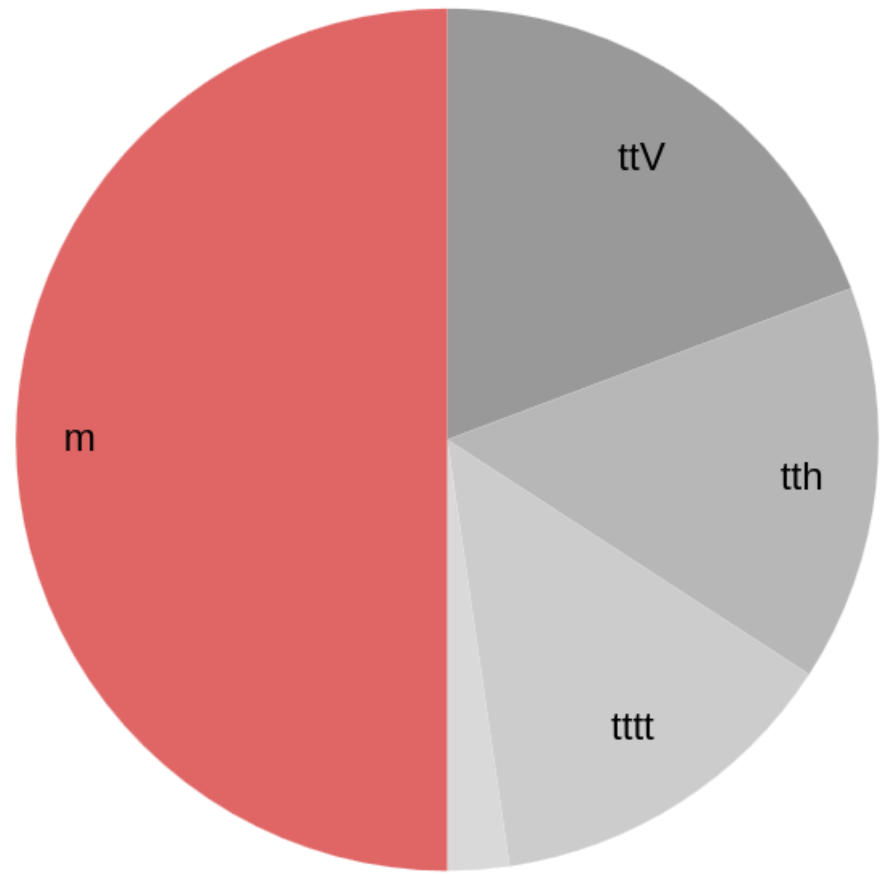

Test

Machine Learning applied to di-boson searches: fermiophilic doubly charged scalars

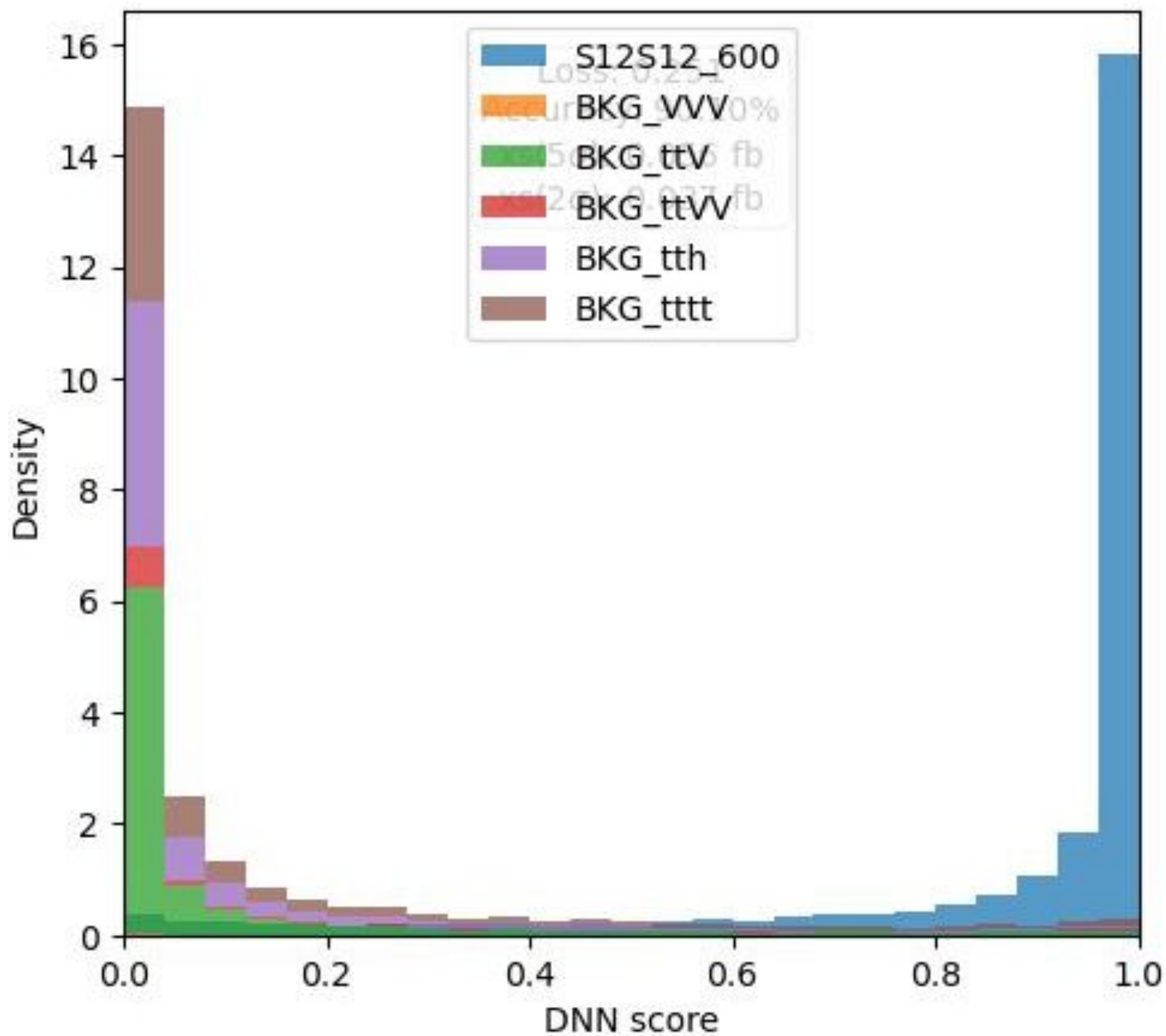

Machine Learning applied to di-boson searches: fermiophilic doubly charged scalars

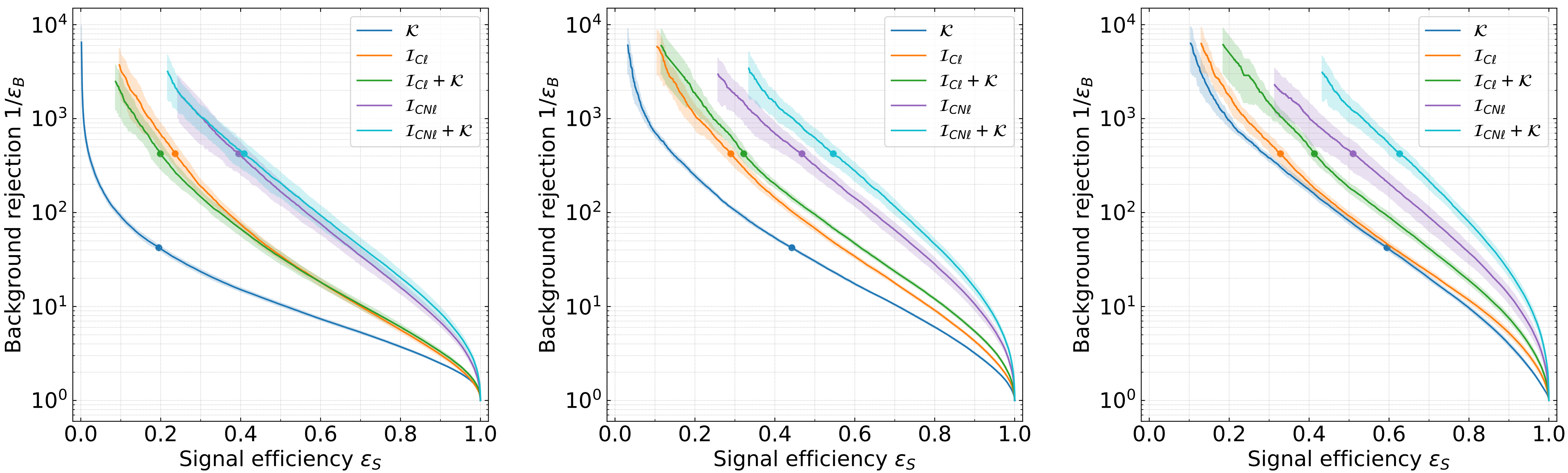

(a) $m_S = 300$ GeV (b) $m_S = 550$ GeV (c) $m_S = 800$ GeV

Figure 5. Comparison of network performances with ROC curves. The markers indicate the working points used in the following analysis.

Machine Learning applied to di-boson searches: fermiophilic doubly charged scalars

LHC
with 3 ab^{-1}

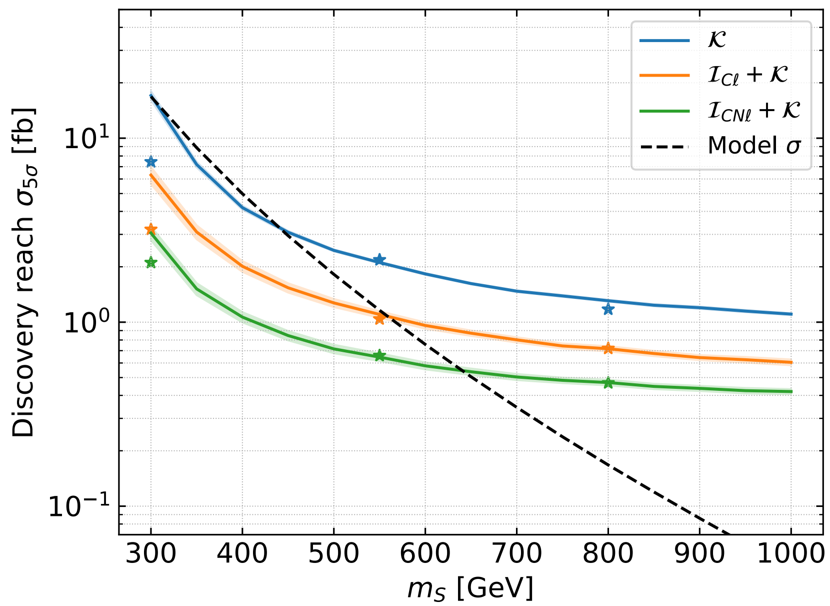

(a) Discovery reach of $S^{++}S^{--}$

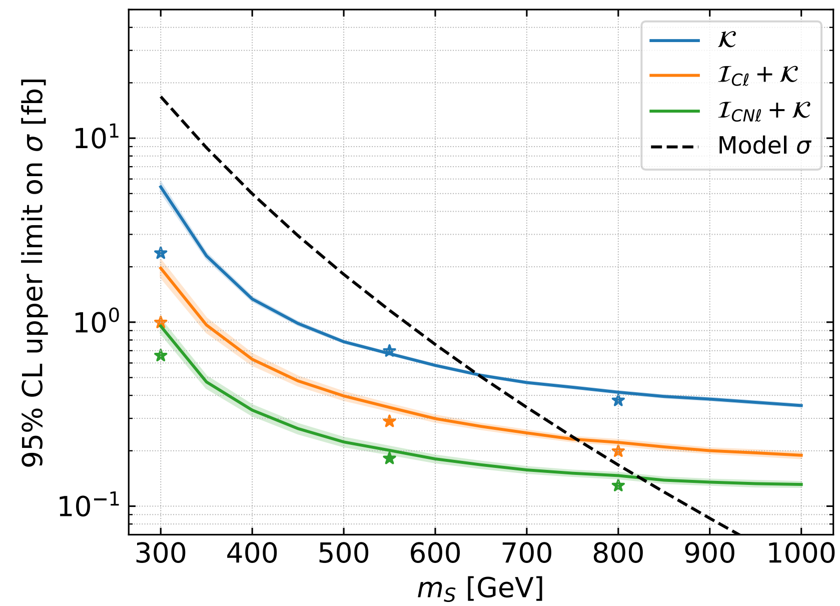

(b) Expected upper limit of $S^{++}S^{--}$

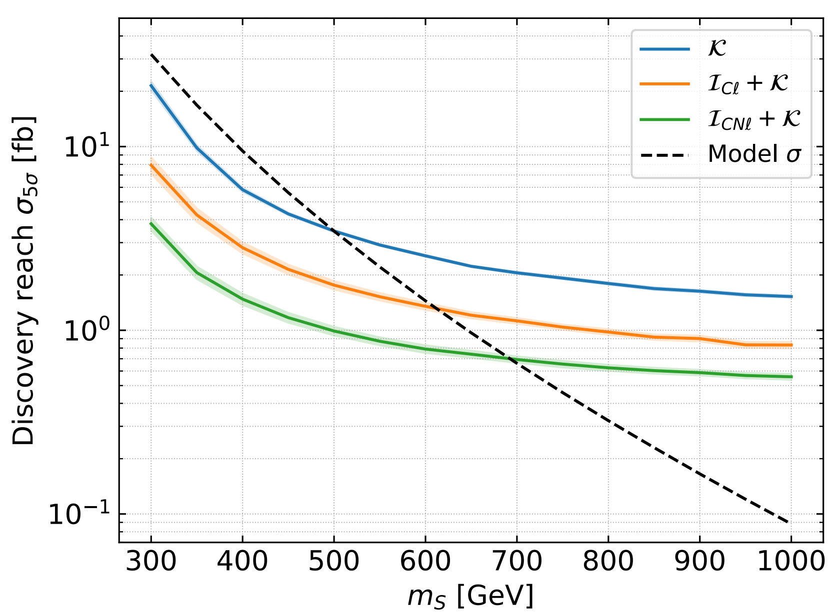

(c) Discovery reach of $S^{++}S^{--}$ and $S^{\pm\pm}S^{\mp}$

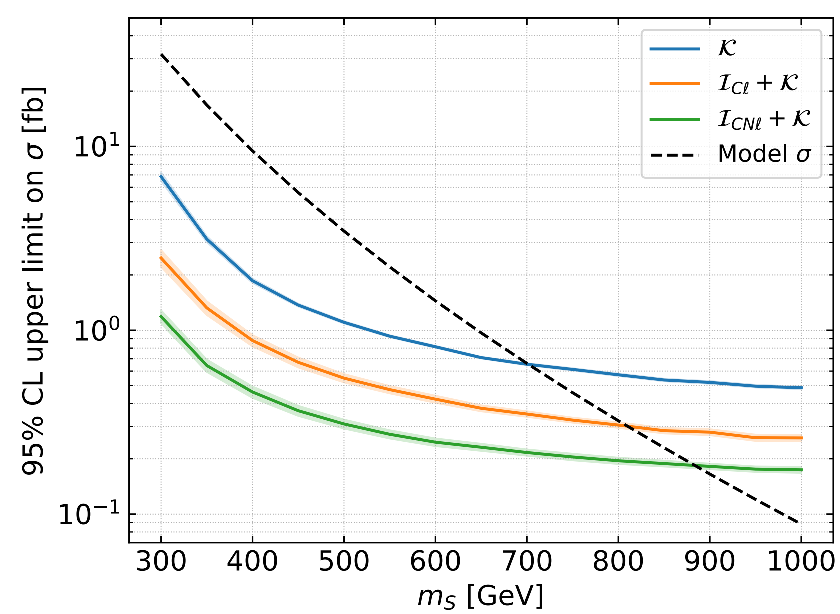

(d) Expected upper limit of $S^{++}S^{--}$ & $S^{\pm\pm}S^{\mp}$

Machine Learning applied to di-boson searches: fermiophilic doubly charged scalars

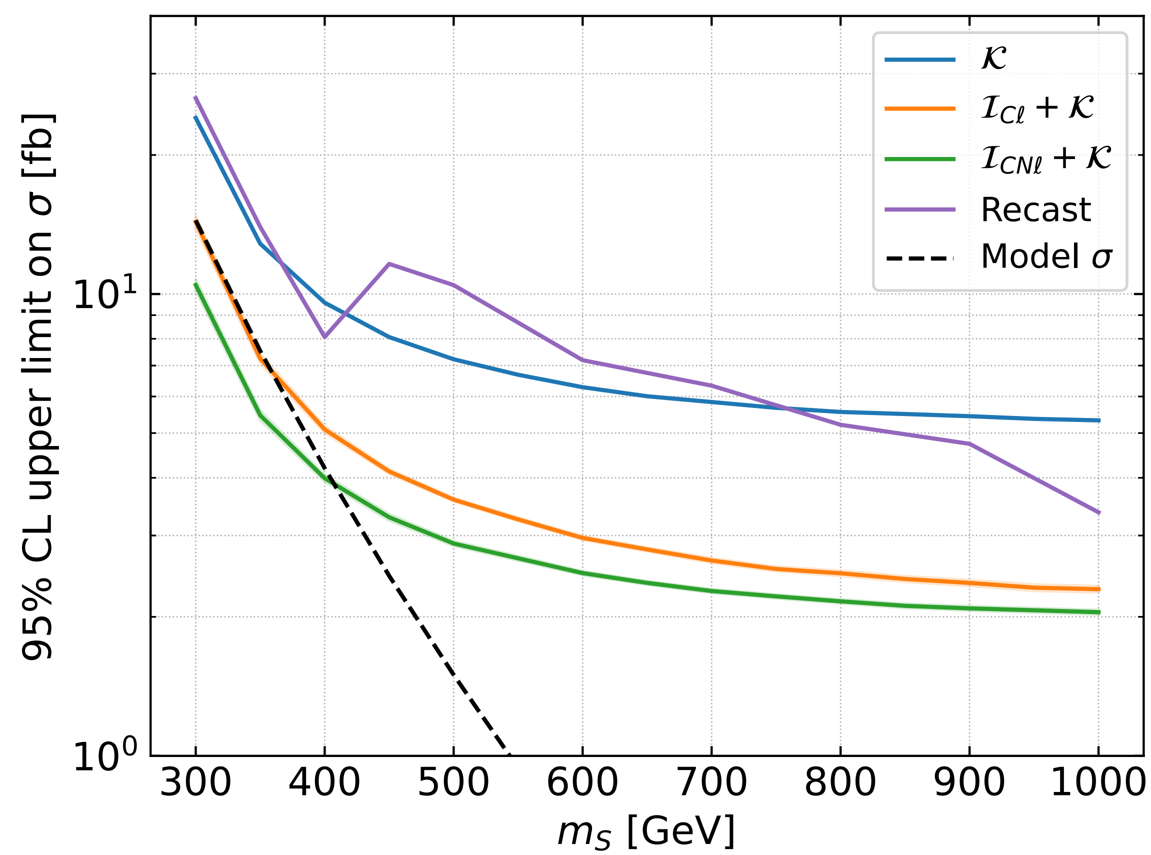

Figure 7. Expected exclusion limit of $S^{++}S^{--}$ pair production at the LHC with $\mathcal{L}_{\rm int} = 139$ fb^{-1} for different network architectures. The recast bounds are taken from Ref. [22]. The black line indicates the 13 TeV reference cross sections in the SU(5)/SO(5) model.

Summary

- Many BSM models predict increased tbWtbW production.
- We presented a detailed search proposal for pair-produced doubly charged scalars in the tbWtbW channel which uses a DNN for signal discrimination.
- Convolutional neural networks using jet images provide excellent performance on this final state with many hadrons.
- Doubly charged scalars can potentially be discovered up to a mass of 640 GeV or excluded up to a mass of 820 GeV by the full 3 ab^{-1} LHC run.
- CNN-based search strategies are applicable to other final states with high hadronic activity.
- See arXiv:2304.09195 for more details.

Backup

Phenomenology of electroweak PNGBs in CHM
Simplified model approach

A simplified model approach to obtain bounds from existing searches:

- We implement a simplified model in FeynRules which features:
  - pseudo- scalars with charge 2, 1, and a scalar and pseudo-scalar with charge 0
  - scalar pair production via Drell-Yan
  - scalar decay into two EW gauge bosons or into 3rd gen. quarks, respecting NWA
- We simulate signal events for each combination of decay channels of two scalars with MadGraph5,
- and determine bounds on production cross section times branching ratio into each channel combination by matching simulated events against all searches and measurements available in MadAnalysis5, CheckMATE and Contur.

Simplified model Lagrangian

$$\mathcal{L}_{\rm int} = \mathcal{L}_{SSV} + \mathcal{L}_{SVV} + \mathcal{L}_{ffS}$$

Production:
(and cascade decays)

$$\begin{aligned}\mathcal{L}_{SSV} = & \frac{ie}{s_W} W^{-\mu}\left(K_W^{S^0 S^+} S^0 \overleftrightarrow{\partial_\mu} S^+ + K_W^{S^{0\prime} S^+} S^{0\prime} \overleftrightarrow{\partial_\mu} S^+ + K_W^{S^- S^{++}} S^- \overleftrightarrow{\partial_\mu} S^{++}\right) + \text{h.c.} \\ & + \frac{ie}{s_W c_W} Z^\mu \left(K_Z^{S^0 S^{0\prime}} S^0 \overleftrightarrow{\partial_\mu} S^{0\prime} + K_Z^{S^+ S^-} S^+ \overleftrightarrow{\partial_\mu} S^- + K_Z^{S^{++} S^{--}} S^{++} \overleftrightarrow{\partial_\mu} S^{--}\right) \\ & - ieA^\mu \left(S^+ \overleftrightarrow{\partial_\mu} S^- + 2S^{++} \overleftrightarrow{\partial_\mu} S^{--}\right) ,\end{aligned}$$

decay
to gauge bosons:

$$\begin{aligned}\mathcal{L}_{SVV} = \frac{e^2}{16\pi^2 v}\Bigg[& S^0\left(\tilde{K}^{S^0}_{\gamma\gamma} F_{\mu\nu}\tilde{F}^{\mu\nu} + \frac{2}{s_W c_W}\tilde{K}^{S^0}_{\gamma Z} F_{\mu\nu}\tilde{Z}^{\mu\nu} + \frac{1}{s_W^2 c_W^2}\tilde{K}^{S^0}_{ZZ} Z_{\mu\nu}\tilde{Z}^{\mu\nu} + \frac{2}{s_W^2}\tilde{K}^{S^0}_{WW} W^+_{\mu\nu}\tilde{W}^{-\mu\nu}\right) \\ & + S^{0\prime}\left(K^{S^{0\prime}}_{\gamma\gamma} F_{\mu\nu}F^{\mu\nu} + \frac{2}{s_W c_W}K^{S^{0\prime}}_{\gamma Z} F_{\mu\nu}Z^{\mu\nu} + \frac{1}{s_W^2 c_W^2}K^{S^{0\prime}}_{ZZ} Z_{\mu\nu}Z^{\mu\nu} + \frac{2}{s_W^2}K^{S^{0\prime}}_{WW} W^+_{\mu\nu}W^{-\mu\nu}\right) \\ & + \left(S^+\left(\frac{2}{s_W}\tilde{K}^{S^+}_{\gamma W} F_{\mu\nu}\tilde{W}^{-\mu\nu} + \frac{2}{s_W^2 c_W}\tilde{K}^{S^+}_{ZW} Z_{\mu\nu}\tilde{W}^{-\mu\nu}\right) + \text{h.c.}\right) \\ & + S^{++}\frac{1}{s_W^2}\tilde{K}^{S^{++}}_{W^-W^-} W^-_{\mu\nu}\tilde{W}^{-\mu\nu} + \text{h.c.}\Bigg] .\end{aligned}$$

decay
to fermions:

$$\begin{aligned}\mathcal{L}_{ffS} = & S^0\left[\bar{t}\left(\kappa_t^{S^0} + i\tilde{\kappa}_t^{S^0}\gamma_5\right)t + \bar{b}\left(\kappa_b^{S^0} + i\tilde{\kappa}_b^{S^0}\gamma_5\right)b\right] + \left(S^0 \to S^{0\prime}\right) \\ & + S^+\,\bar{t}\left(\kappa^{S^+}_{tb,L}P_L + \kappa^{S^+}_{tb,R}P_R\right)b + \text{h.c.} ,\end{aligned}$$

pair decay channels (fermion-phobic scenario)

fermiophobic	$S^{++}S^{--}$	$S^{\pm\pm}S^{\mp}$	$S^{+}S^{-}$	$S^{\pm}S^{0(\prime)}$	$S^{0}S^{0\prime}/S^{0\prime}S^{0}$
$WWWW$	$W^+W^+W^-W^-$	-	-	-	$W^+W^-W^+W^-$
$WWW\gamma$	-	$W^\pm W^\pm W^\mp\gamma$	-	$W^\pm\gamma W^+W^-$	-
$WWWZ$	-	$W^\pm W^\pm W^\mp Z$	-	$W^\pm ZW^+W^-$	-
$WW\gamma\gamma$	-	-	$W^+\gamma W^-\gamma$	-	$W^+W^-\gamma\gamma$
$WWZ\gamma$	-	-	$W^\pm\gamma W^\mp Z$	-	$W^+W^-\gamma Z$
$WWZZ$	-	-	W^+ZW^-Z	-	W^+W^-ZZ
$W\gamma\gamma\gamma$	-	-	-	$W^\pm\gamma\gamma\gamma$	-
$WZ\gamma\gamma$	-	-	-	$W^\pm\{Z\gamma\}\gamma$	-
$WZZ\gamma$	-	-	-	$W^\pm\{Z\gamma\}Z$	-
$WZZZ$	-	-	-	$W^\pm ZZZ$	-
$\gamma\gamma\gamma\gamma$	-	-	-	-	$\gamma\gamma\gamma\gamma$
$Z\gamma\gamma\gamma$	-	-	-	-	$Z\gamma\gamma\gamma$
$ZZ\gamma\gamma$	-	-	-	-	$Z\{Z\gamma\}\gamma$
$ZZZ\gamma$	-	-	-	-	$ZZZ\gamma$
$ZZZZ$	-	-	-	-	$ZZZZ$

Table 1: Classification of the 24 di-scalar channels in terms of the 5 pair production cases (columns) and the 15 combinations of gauge bosons (rows) from decays. In the channels, the first two and second two bosons are resonantly produced. The notation $\{Z\gamma\} = Z\gamma + \gamma Z$ indicates the two permutations. Charge-conjugated states belong to the same di-scalar channel.

pair decay channels (fermion-phobic scenario)

fermiophilic	$S^{++}S^{--}$	$S^{++}S^{-}$	$S^{+}S^{-}$	$S^{+}S^{0(\prime)}$	$S^{0}S^{0\prime}/S^{0\prime}S^{0}$
$tttt$	-	-	-	-	$t\bar{t}t\bar{t}$
$tttb$	-	-	-	$t\bar{b}t\bar{t}$	-
$ttbb$	-	-	$t\bar{b}b\bar{t}$	-	$t\bar{t}b\bar{b}$
$tbbb$	-	-	-	$t\bar{b}b\bar{b}$	-
$bbbb$	-	-	-	-	$b\bar{b}b\bar{b}$
$Wttbb$	-	$W^{+}t\bar{b}b\bar{t}$	-	-	-
$WWttbb$	$W^{+}t\bar{b}W^{-}b\bar{t}$	-	-	-	-

Table 2: Classification of the 8 di-scalar channels in terms of the 5 pair production cases (columns) and the 5 combinations of top and bottom from decays (rows). In cases with one or two doubly charged scalars, one always obtains $ttbb$ with one or two additional W's, respectively. The charge-conjugated states are not shown.

…just for orientation

Typical Drell-Yan production cross sections (in SU(5)→SO(5) models):

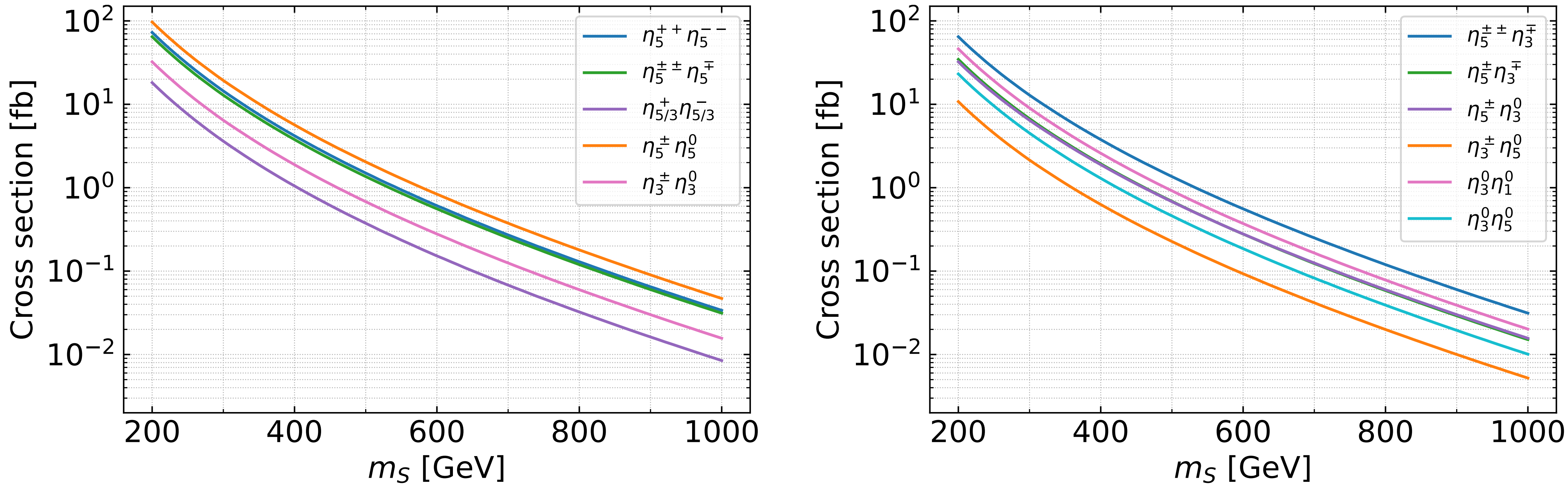

Figure 3: Cross sections for the Drell-Yan production of SU(5)/SO(5) pNGBs at the LHC with $\sqrt{s} = 13\,\text{TeV}$, assuming the same mass for all states of the custodial singlet, triplet, and quintuplet. Note that the $\eta_1^0\eta_5^0$ combination is not allowed as they are both parity-odd.

EW scalar pairs: bounds from the LHC

Model agnostic bounds: (**can be used for ANY model with dominant DY production**)

We simulate Drell-Yan pair production of EW pNGBs and decays into various decay channels and determine bounds from searches available in event-recast data bases.
(Simulaton chain: Feynrules → Madgraph5 → Pythia8 → (→ Delphes →) MadAnalysis5/ CheckMATE/Contur)

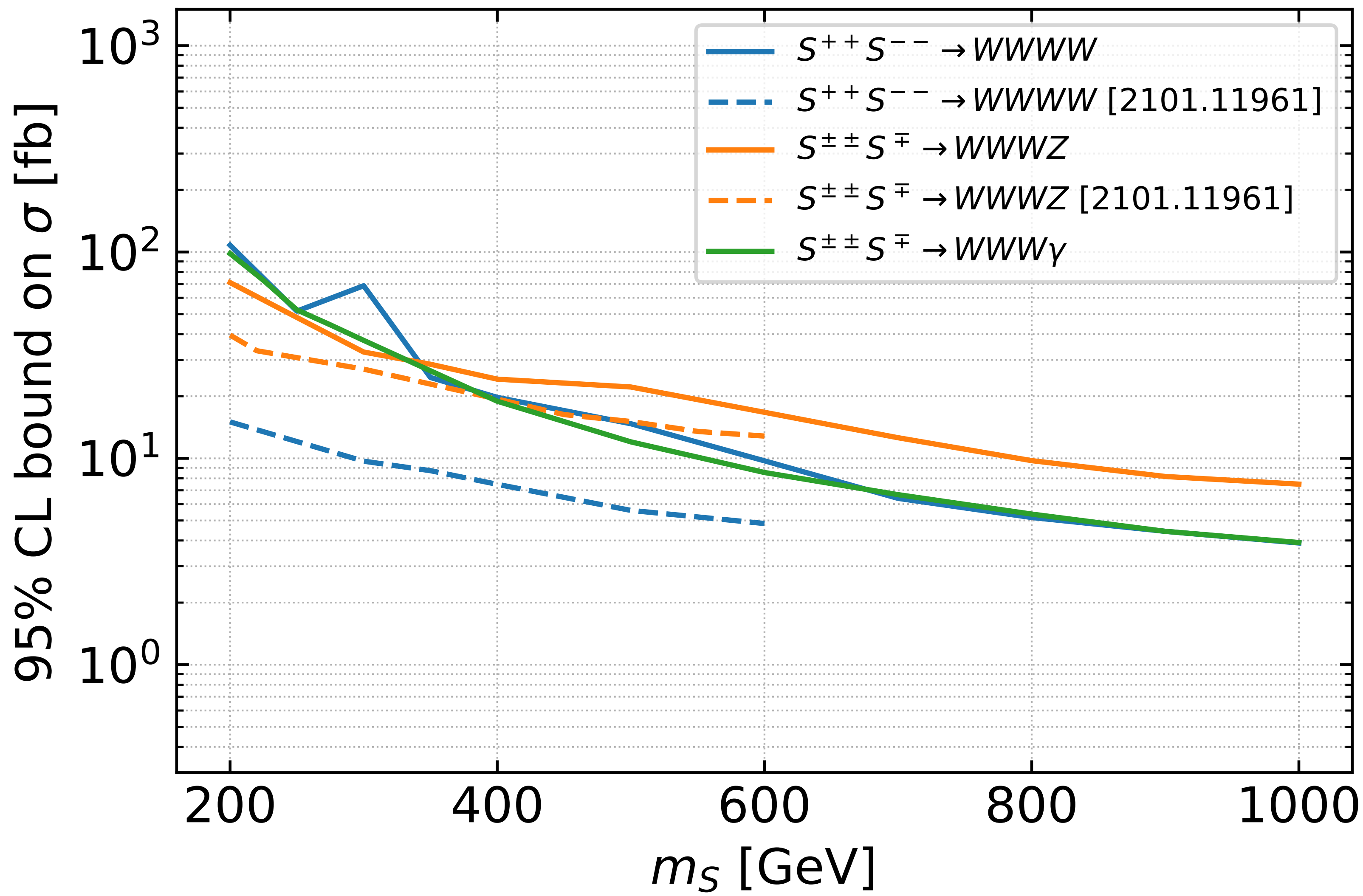

(b) $S^{++}S^{--}$ and $S^{\pm\pm}S^{\mp}$ with di-boson decays

EW scalar pairs: bounds from the LHC

Model agnostic bounds: (**can be used for ANY model with dominant DY production**)

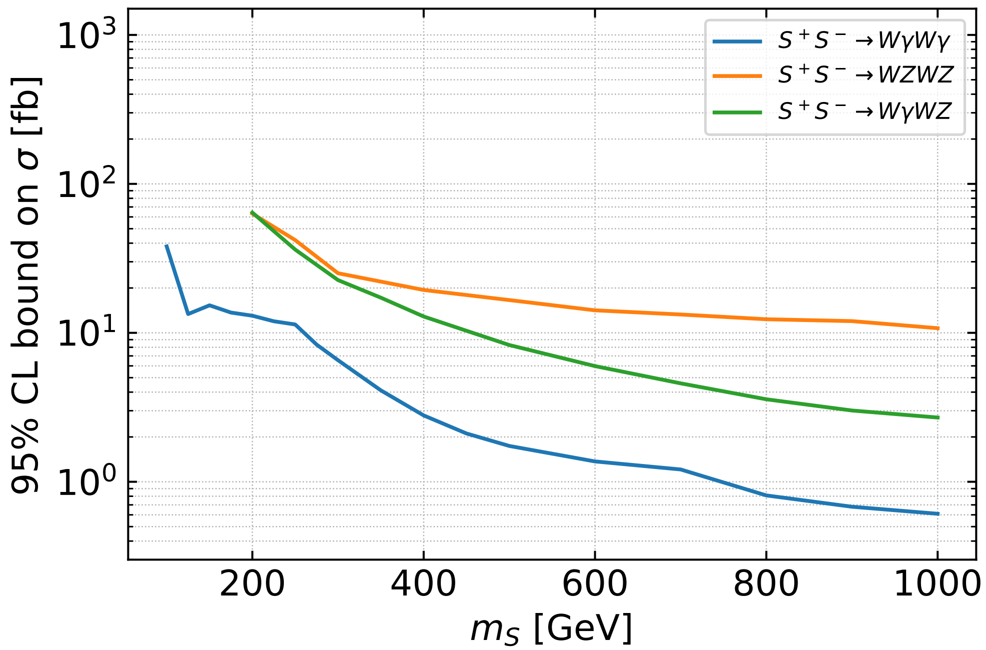

(c) S^+S^- with di-boson decays

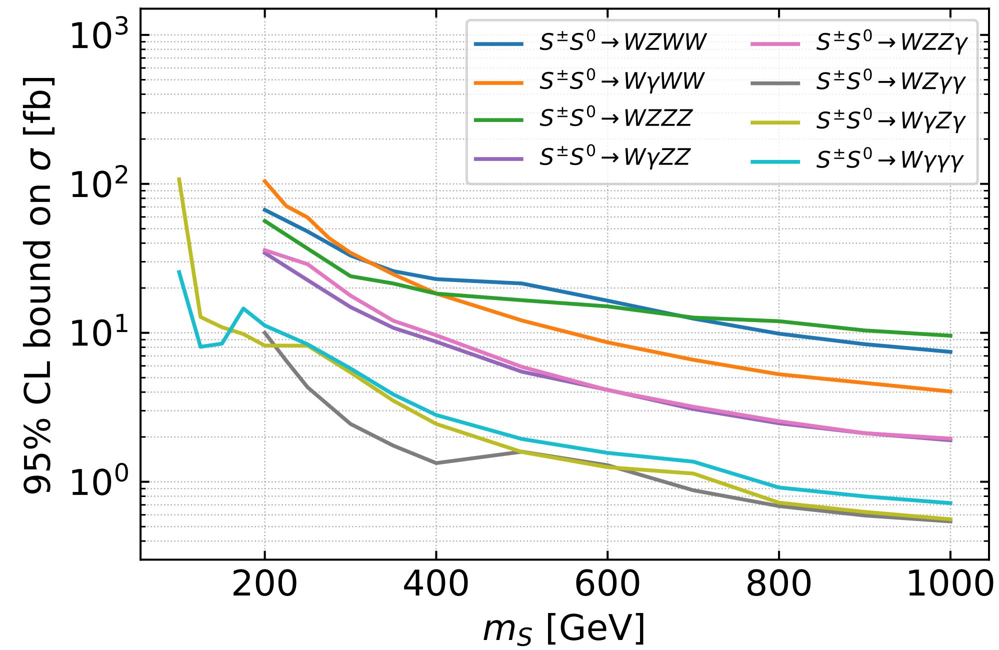

(d) $S^\pm S^0$ with di-boson decays

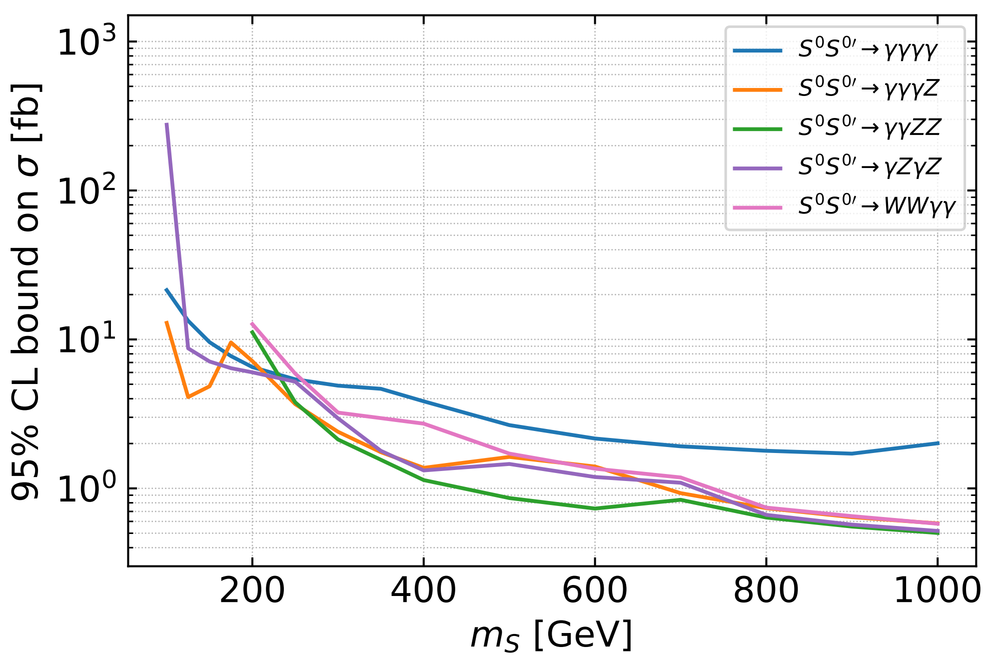

(e) $S^0S^{0\prime}$ with di-boson decays with ≥ 2 photons

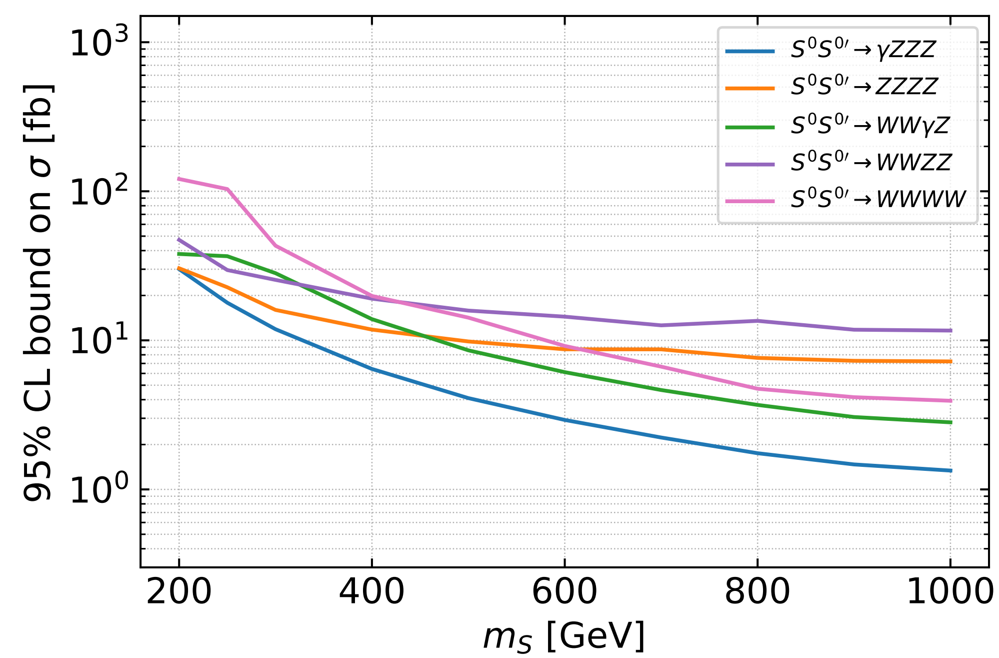

(f) $S^0S^{0\prime}$ with di-boson decays with ≤ 1 photons

EW scalar pairs: bounds from the LHC

Model agnostic bounds: (**can be used for ANY model with dominant DY production**)

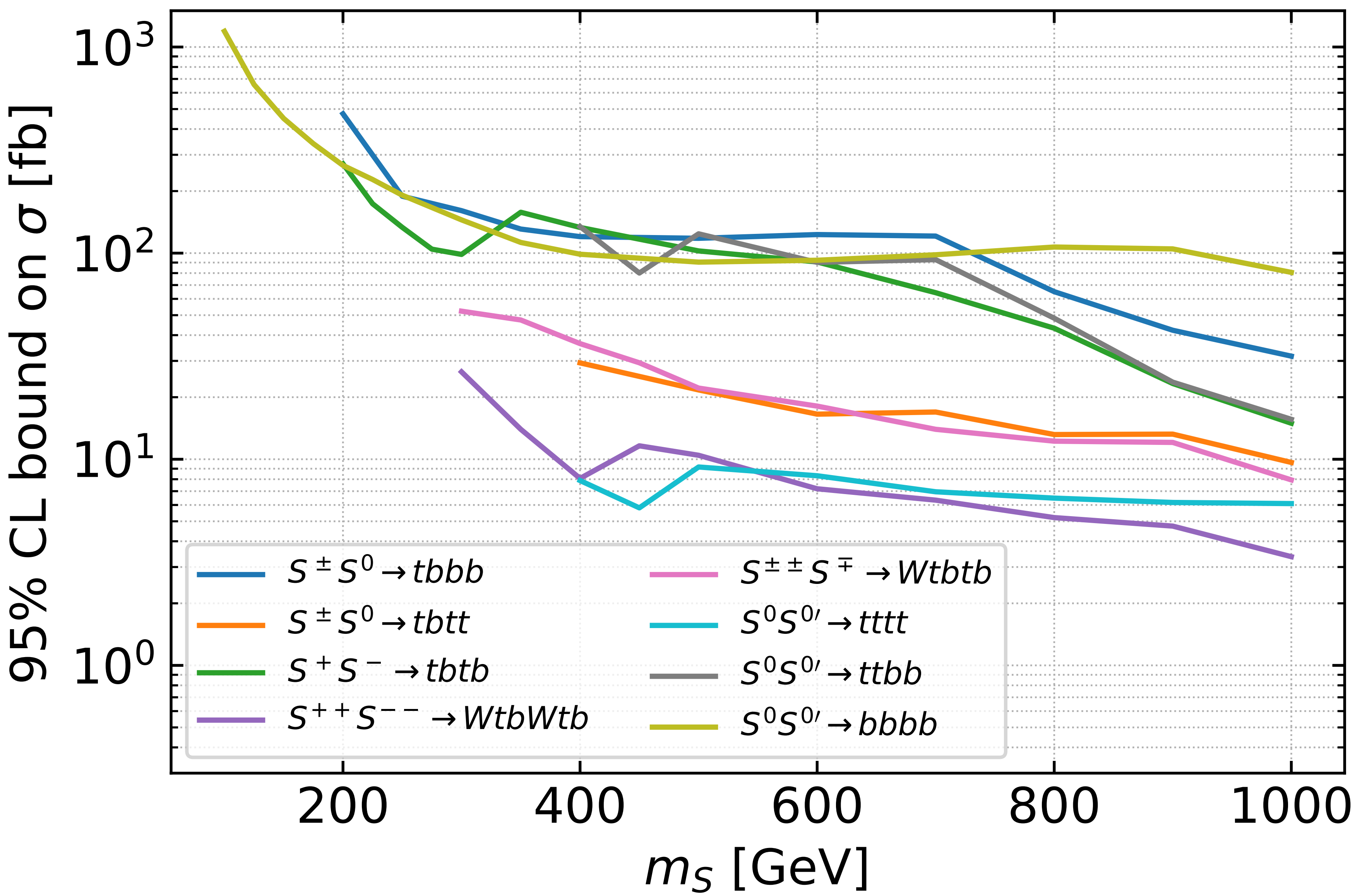

(a) Scalar pair with decays to quarks

There is a lot of room for improvement in many diboson channels

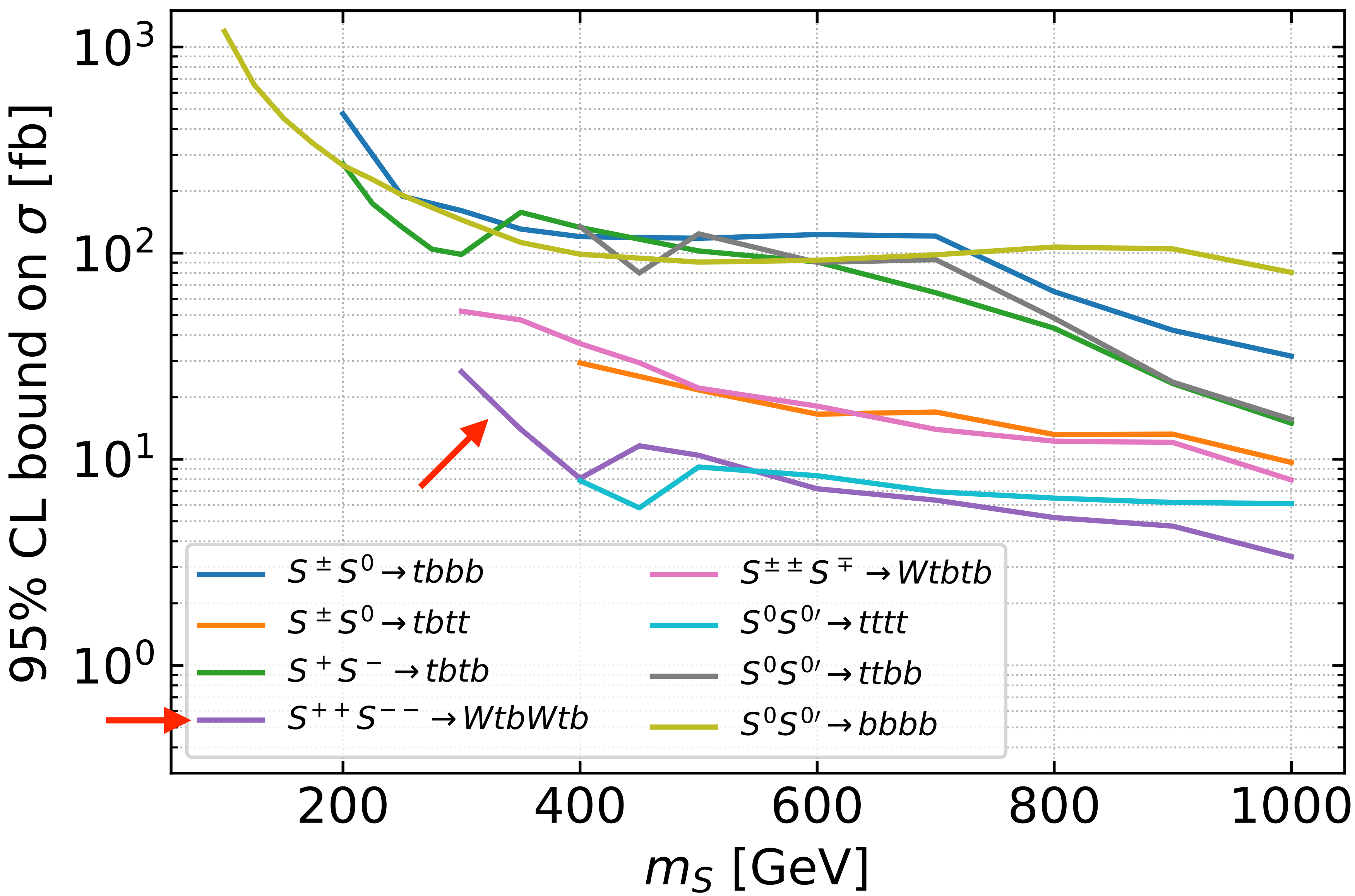

(a) Scalar pair with decays to quarks

CH: EW pNGBs - bounds from the LHC

EW sector: SU(5)→SO(5)

- 14 pNGBs in a (3,3), a (2,2) and a (1,1) of $SU(2)_L \times SU(2)_R$
  an EW singlet, the Higgs, and $(\mathbf{3},\mathbf{3}) \to \mathbf{5} + \mathbf{3} + \mathbf{1} \equiv \eta_5 + \eta_3 + \eta_1\,,$
  $$\eta_5 = (\eta_5^{++}, \eta_5^{+}, \eta_5^{0}, \eta_5^{-}, \eta_5^{--}), \quad \eta_3 = (\eta_3^{+}, \eta_3^{0}, \eta_3^{-}), \quad \eta_1 = \eta_1^0$$
- Couplings:
  SS'V: gauge interactions (fixed; relevant for production; or cascade decays)
  SVV': WZW interactions (tiny; relevant for decay)
  Sff': explicit symmetry breaking terms (tiny; relevant for decay)
- Single-production of EW pNGBs is strongly suppressed.
- Pair-production is generically dominated by Drell-Yan pair production.
- For a given model, the WZW coefficients are fixed, and thus branching fractions of pNGB decays to EW gauge bosons are determined.
- Decays to 3rd generation quarks arise from a different source.
- Typically dominant pNGB decay channels:

fermiophilic scenario

$$\eta_5^{++} \to W^+ t\bar{b}$$
$$\eta_{3,5}^{+} \to t\bar{b}$$
$$\eta_{1,3,5}^{0} \to t\bar{t},\ b\bar{b}$$

fermiophobic scenario

$$\eta_5^{++} \to W^+ W^+$$
$$\eta_{3,5}^{+} \to W^+\gamma,\ W^+ Z$$
$$\eta_{1,5}^{0} \to \gamma\gamma,\ \gamma Z,\ ZZ$$
$$\eta_3^0 \to W^+W^-\gamma,\ W^+W^-Z \qquad \text{via } \eta_{3,5}^{\pm(*)}$$
$$\eta_3^0 \to Z\gamma\gamma,\ ZZ\gamma,\ ZZZ \qquad \text{via } \eta_{1,5}^{0(*)}$$

CH: EW pNGBs - bounds from the LHC

Production cross sections in SU(5)→SO(5) models:

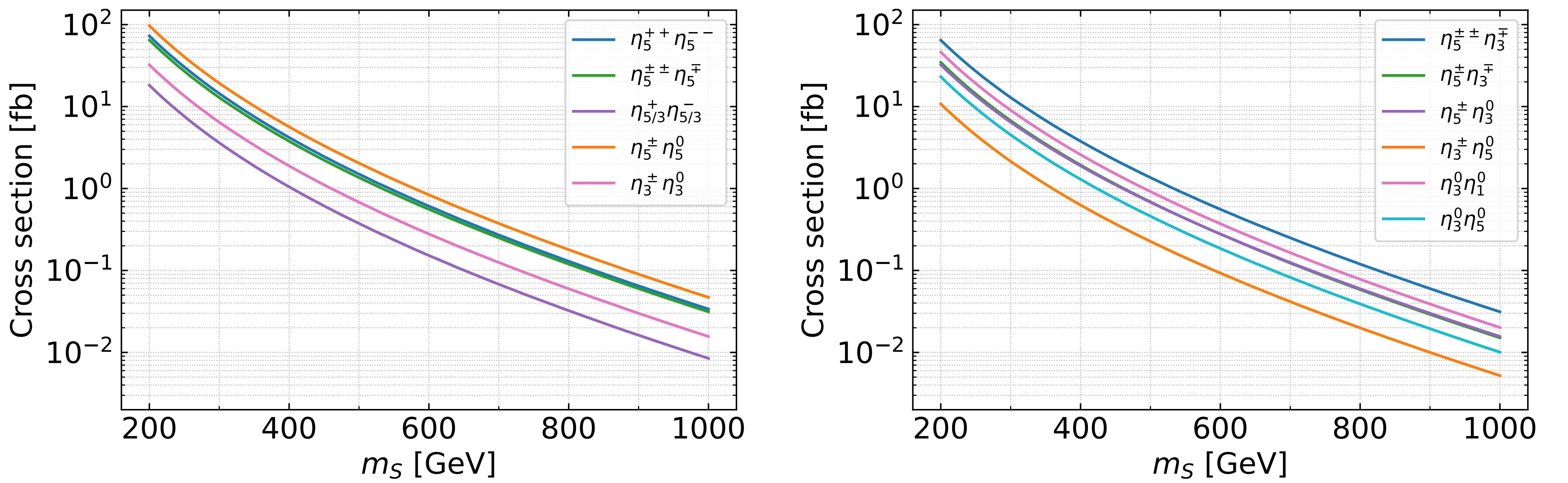

Figure 3: Cross sections for the Drell-Yan production of SU(5)/SO(5) pNGBs at the LHC with $\sqrt{s} = 13\,\text{TeV}$, assuming the same mass for all states of the custodial singlet, triplet, and quintuplet. Note that the $\eta_1^0\eta_5^0$ combination is not allowed as they are both parity-odd.

CH: EW pNGBs - bounds from the LHC

Branching fractions in SU(5)→SO(5) models (fermio-phobic scenario):

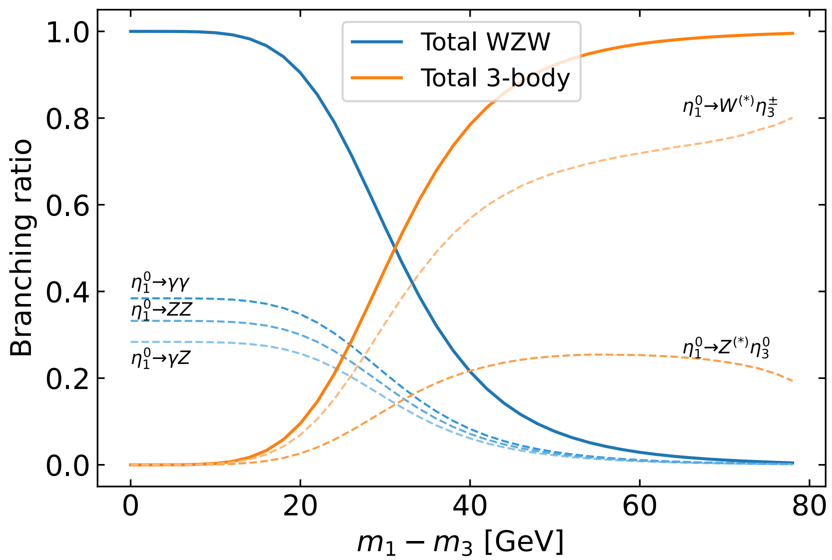

(a) Decays of η_1^0 for $m_1 = 600$ GeV $> m_3$

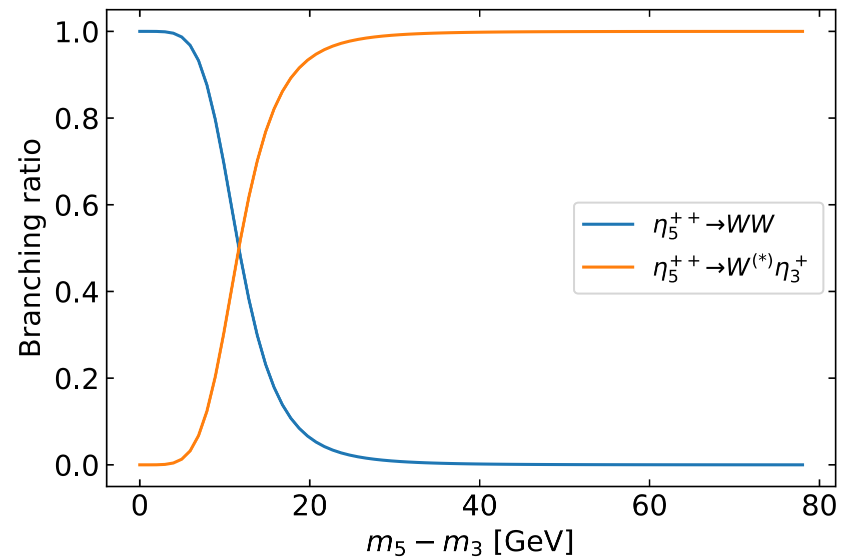

(b) Decays of η_5^{++} for $m_5 = 600$ GeV $> m_3$

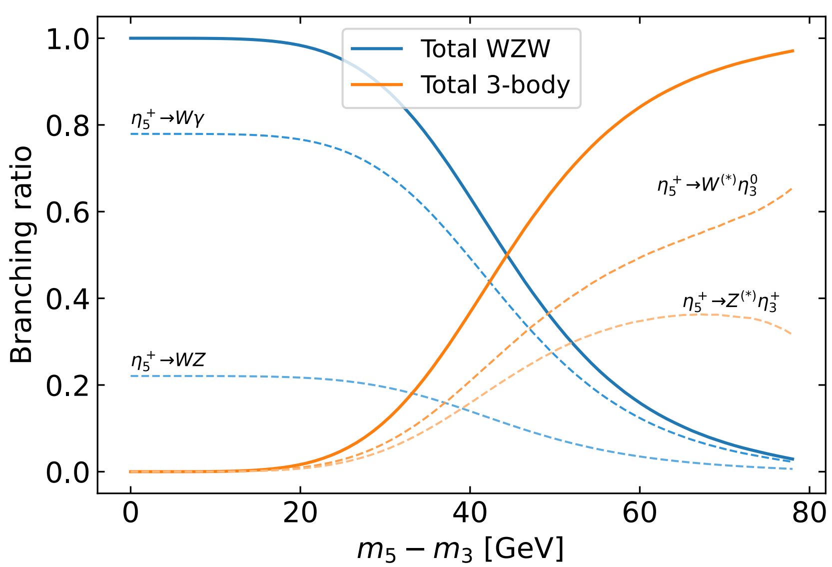

(c) Decays of η_5^+ for $m_5 = 600$ GeV $> m_3$

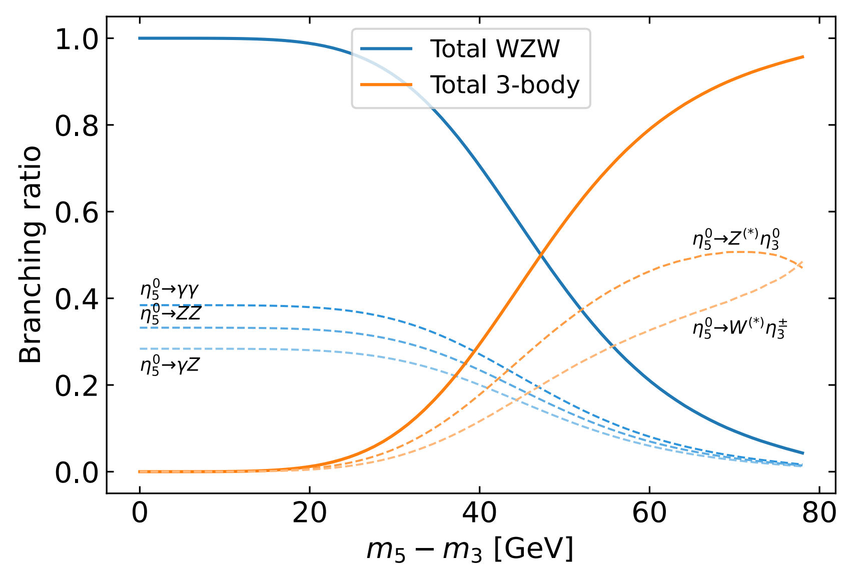

(d) Decays of η_5^0 for $m_5 = 600$ GeV $> m_3$

Figure 5: Overview of the pNGB decays in the fermiophobic case. The mass of the decaying particles is set to 600 GeV. The heavier state decays either via the anomaly into di-boson final states or via an (off-shell) gauge boson into a lighter pNGB.

CH: EW pNGBs - bounds from the LHC

Branching fractions in SU(5)→SO(5) models (fermio-phobic scenario):

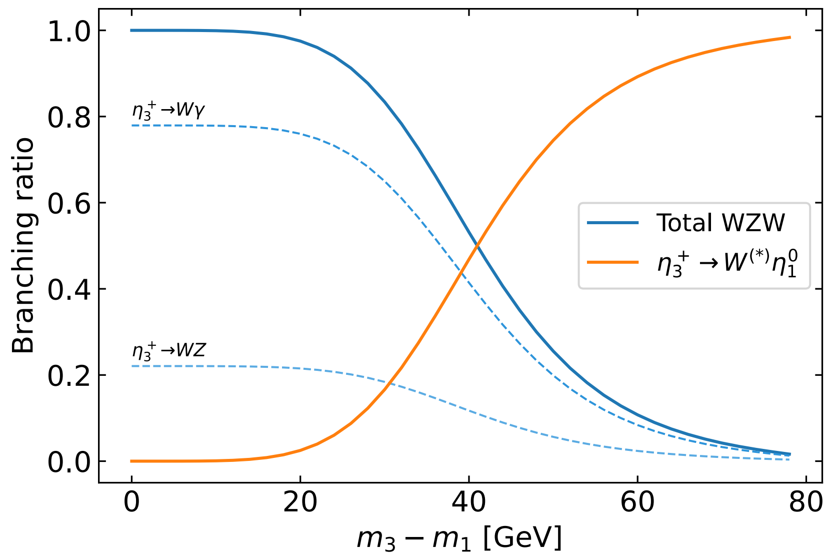

(a) Decays of η_3^+ for $m_5 \gg m_3 = 600$ GeV $> m_1$

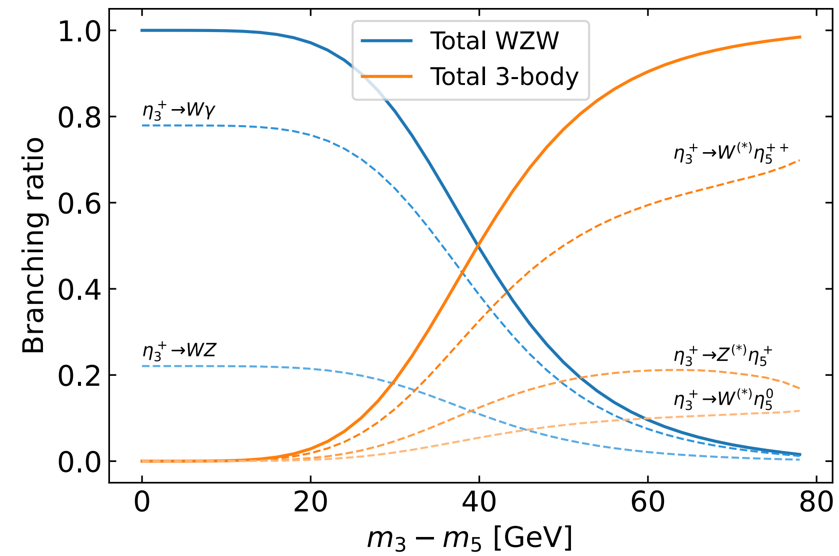

(b) Decays of η_3^+ for $m_1 \gg m_3 = 600$ GeV $> m_5$

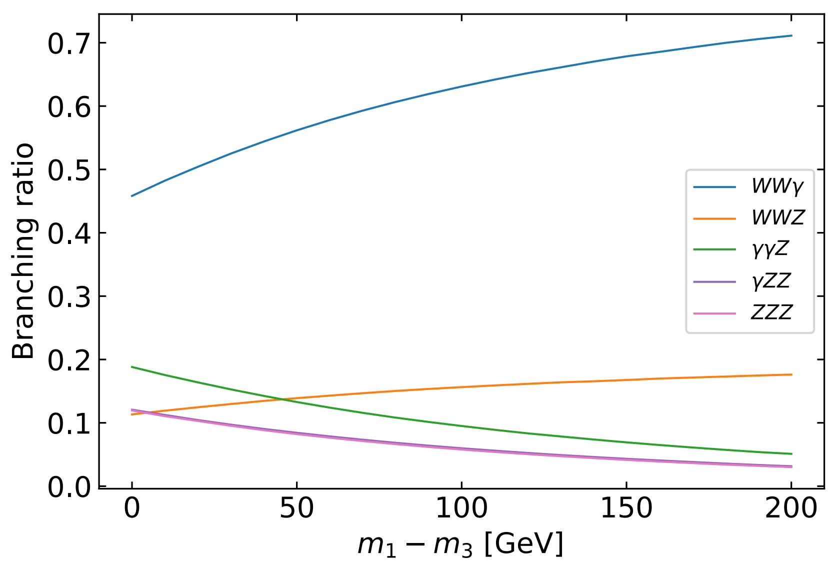

(c) Decays of η_3^0 for $m_5 \gg m_1 > m_3 = 600$ GeV

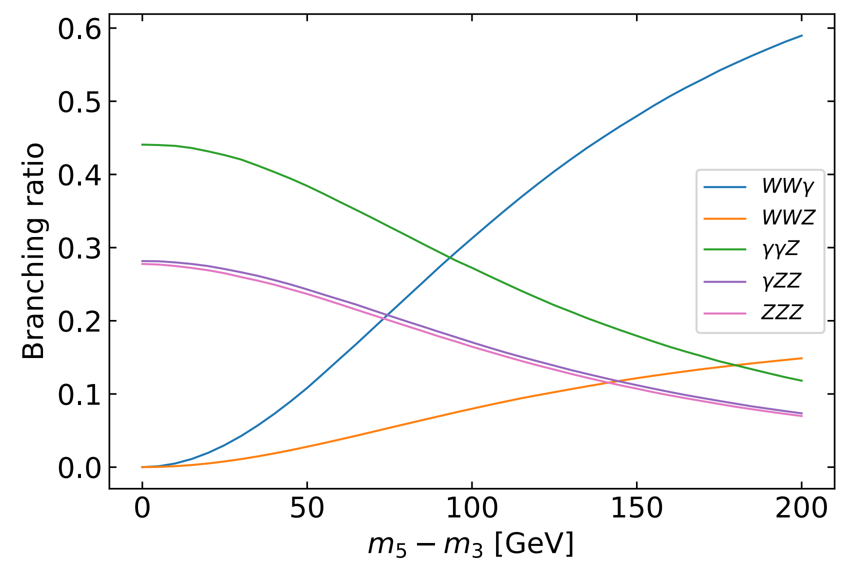

(d) Decays of η_3^0 for $m_1 \gg m_5 > m_3 = 600$ GeV

Figure 6: Overview of the pNGB decays in the fermiophobic case (continued from Fig. 5). The neutral triplet component decays into three gauge bosons, as it does not couple to the anomaly.

CH: EW pNGBs - bounds from the LHC

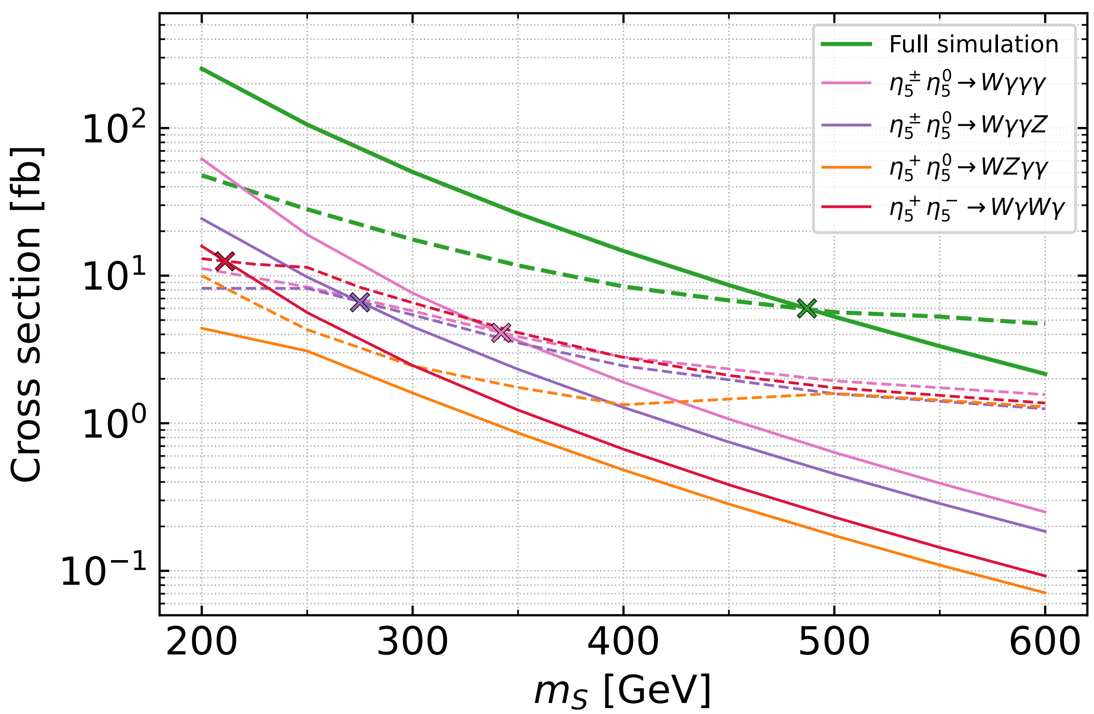

(a) Bounds from individual channels

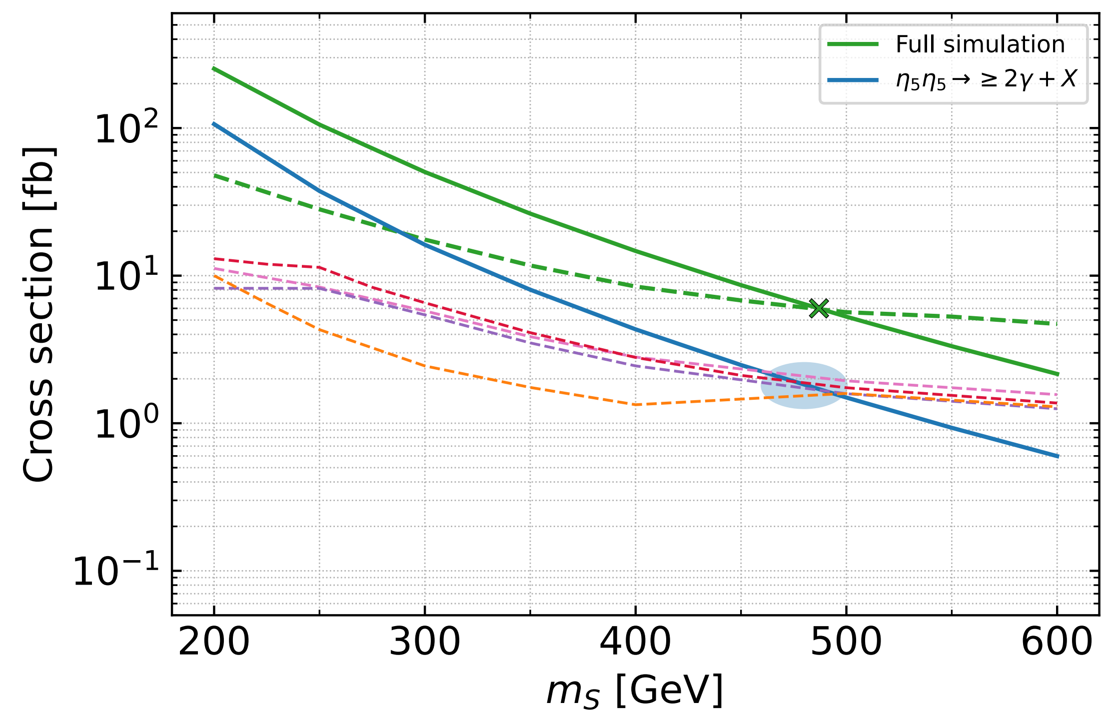

(b) Bounds from sum of multiphoton channels

Figure 7: Application of the model-independent bounds to a specific model, the custodial quintuplet η_5 from the SU(5)/SO(5) coset. In (a) we determine the bounds from the dominant individual channels by comparing the cross section time branching ratio from the model (solid) with the upper limits from Fig. 2 (dashed). In green we show the results of a full simulation. The blue line in (b) is the sum of the individual multi-photon cross sections shown in (a). Further details are given in the text.

CH: EW pNGBs - bounds from the LHC

Resulting bounds in full SU(5)→SO(5) model scenarios

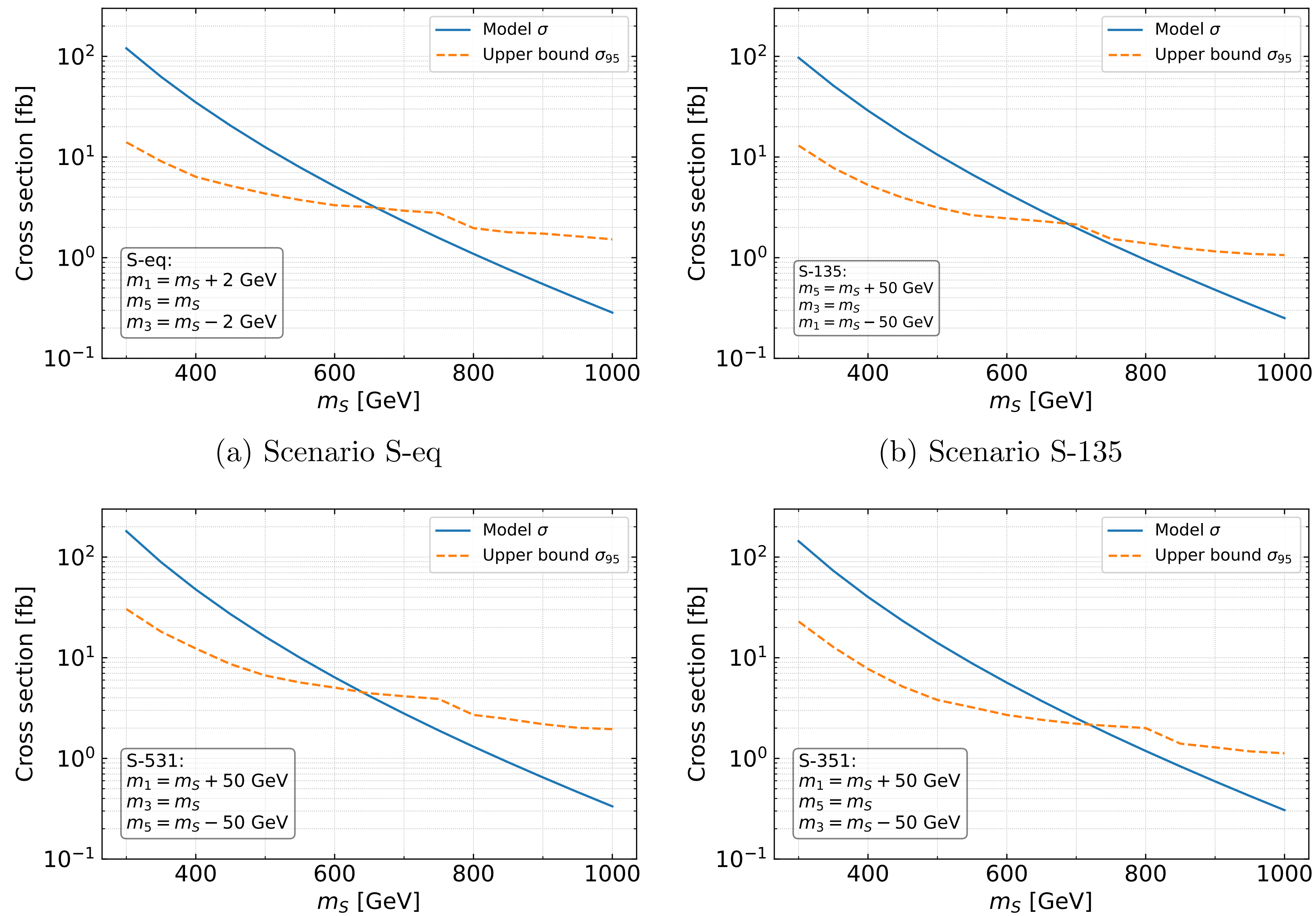

(a) Scenario S-eq

(b) Scenario S-135

(c) Scenario S-531

(d) Scenario S-351

Figure 8: Bounds on the pNGB masses for the Drell-Yan production of the full bi-triplet for multiple benchmark mass spectra defined in Eq. (3.12). In (a), all masses are approximately equal. In the remaining panels, there is a 50 GeV mass split between the multiplets.

Machine Learning applied to di-boson searches: fermiophilic doubly charged scalars

When calculating the 2σ exclusion bound [74], we require:

$$Z_{\rm exc} \equiv \sqrt{-2\,\ln\left(\frac{L(S+B|B)}{L(B|B)}\right)} \geq 1.64, \qquad \text{with} \quad L(x|n) = \frac{x^n}{n!}e^{-x}\,, \tag{5.1}$$

where $L(x|n)$ is the likelihood of observing n events when x events were expected, and S and B are the number of signal and background events, respectively. For achieving a 5σ expected discovery reach, we require

$$Z_{\rm dis} \equiv \sqrt{-2\,\ln\left(\frac{L(B|S+B)}{L(S+B|S+B)}\right)} \geq 5\,. \tag{5.2}$$

Machine Learning applied to di-boson searches: fermiophilic doubly charged scalars

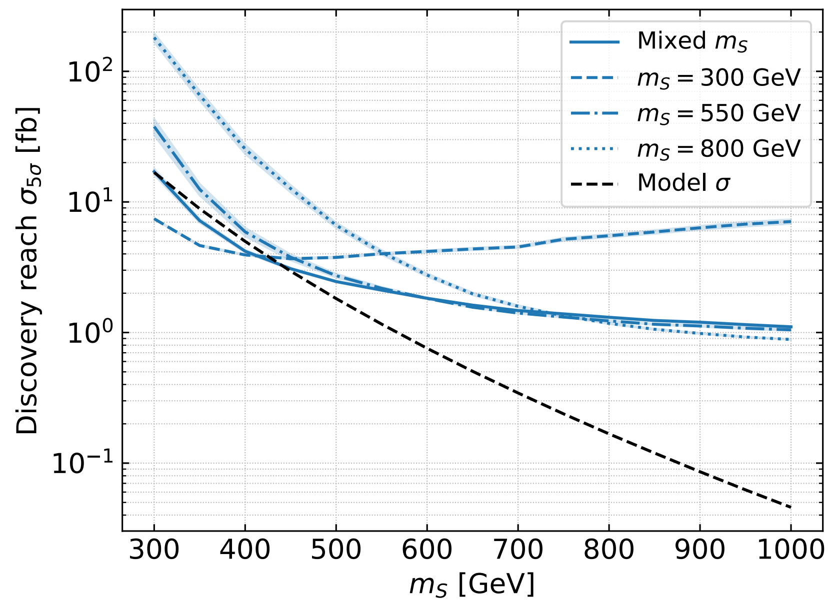

(a) Network $\mathcal{K}$

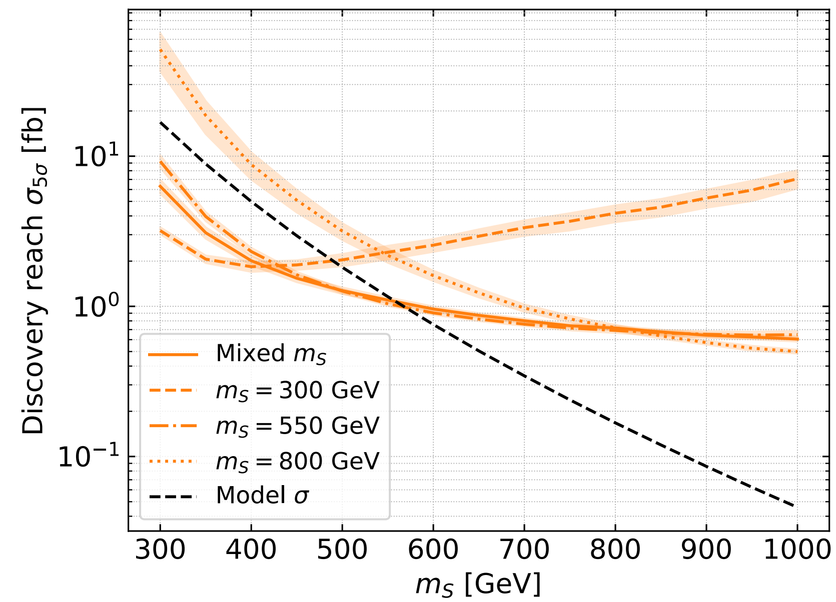

(b) Network $\mathcal{I}_{C\ell} + \mathcal{K}$

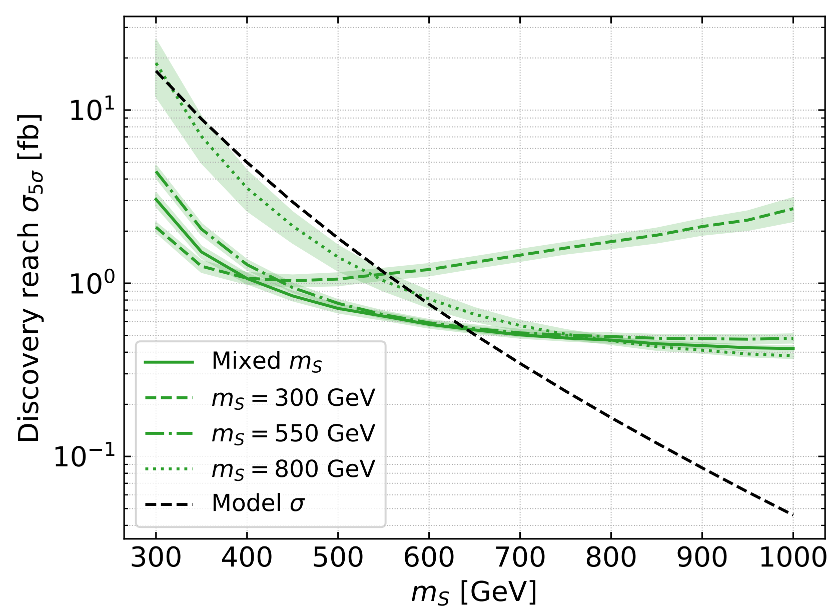

(c) Network $\mathcal{I}_{CN\ell} + \mathcal{K}$

Figure 12. Comparison of networks trained on a single fixed mass.

Machine Learning applied to di-boson searches: fermiophilic doubly charged scalars

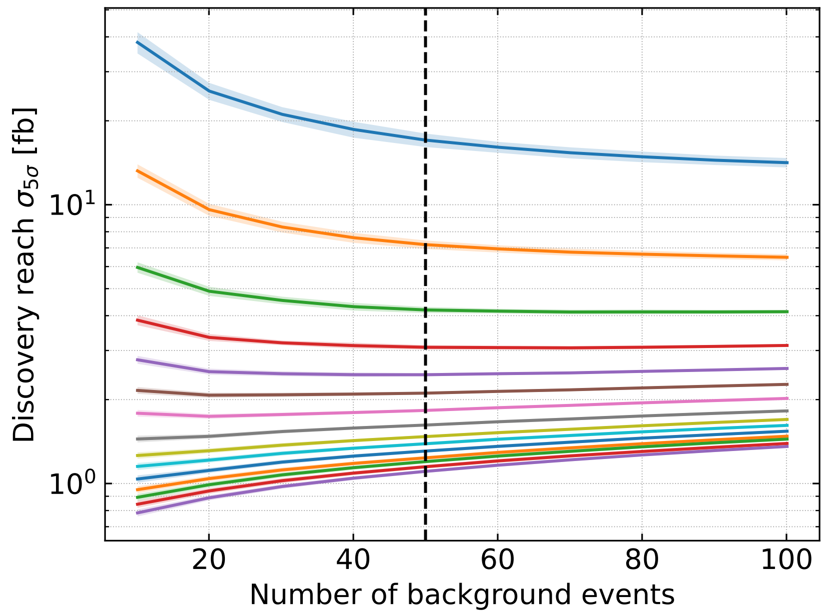

(a) Network $\mathcal{K}$

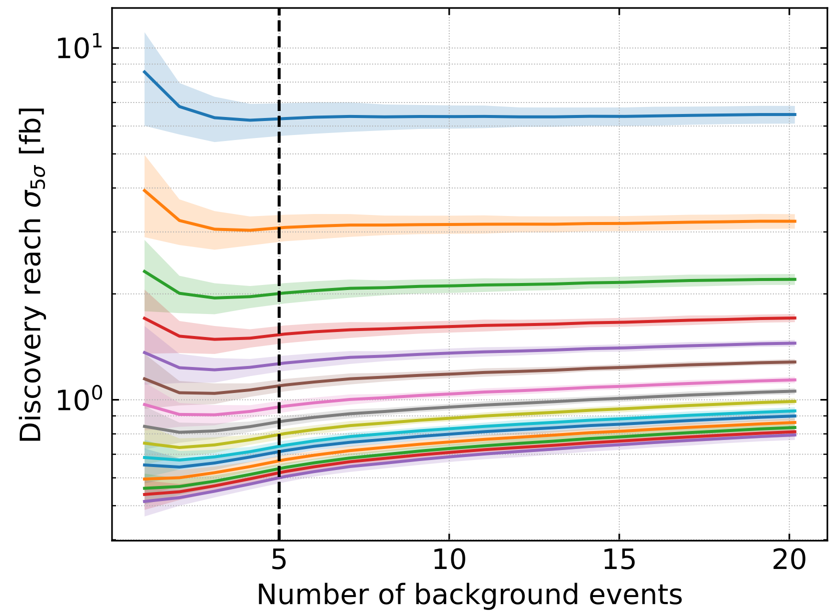

(b) Network $\mathcal{I}_{C\ell} + \mathcal{K}$

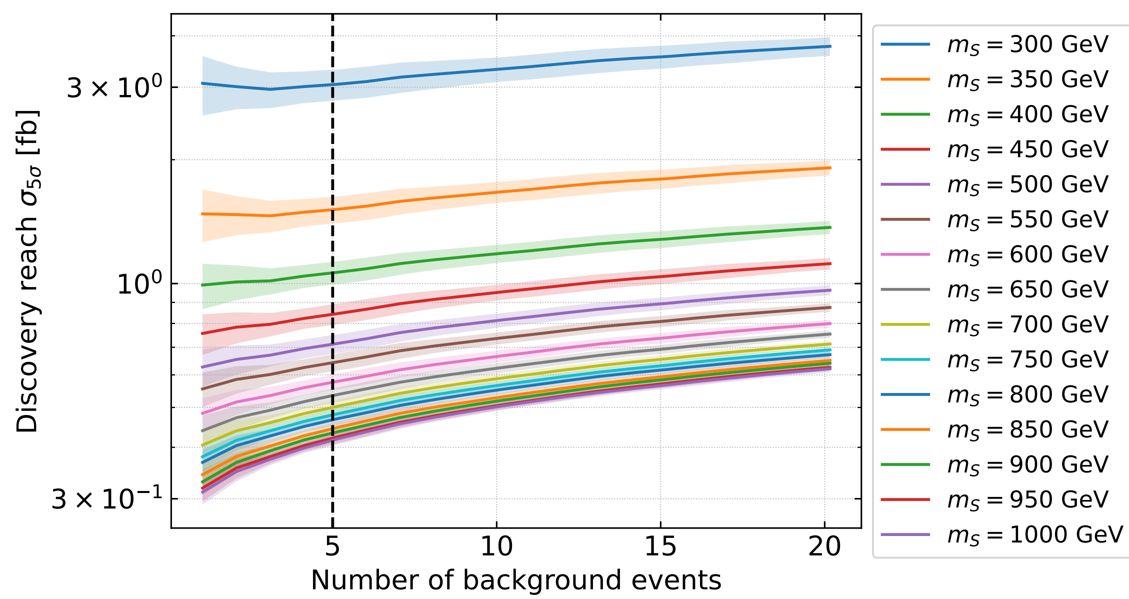

(c) Network $\mathcal{I}_{CN\ell} + \mathcal{K}$

Figure 13. Discovery reach as a function of number of background events, i.e. the NN score cut.